NAVAL POSTGRADUATE SCHOOL

MONTEREY, CALIFORNIA

THESIS

STABILITY ANALYSIS OF A TOWED BODY FOR SHIPBOARD UNMANNED SURFACE VEHICLE RECOVERY

by

Scott D. Roberts

March 2005

Thesis Advisor:	Fotis Papoulias
Second Reader:	William Solitario

THIS PAGE INTENTIONALLY LEFT BLANK

REPORT DOCUMENTATION PAGE			*Form Approved OMB No. 0704-0188*
Public reporting burden for this collection of information is estimated to average 1 hour per response, including the time for reviewing instruction, searching existing data sources, gathering and maintaining the data needed, and completing and reviewing the collection of information. Send comments regarding this burden estimate or any other aspect of this collection of information, including suggestions for reducing this burden, to Washington headquarters Services, Directorate for Information Operations and Reports, 1215 Jefferson Davis Highway, Suite 1204, Arlington, VA 22202-4302, and to the Office of Management and Budget, Paperwork Reduction Project (0704-0188) Washington DC 20503.			
1. AGENCY USE ONLY *(Leave blank)*	2. REPORT DATE March 2005	3. REPORT TYPE AND DATES COVERED Master's Thesis	
4. TITLE AND SUBTITLE: Stability Analysis of a Towed Body for Shipboard Unmanned Surface Vehicle Recovery			5. FUNDING NUMBERS
6. AUTHOR(S) Scott D. Roberts			
7. PERFORMING ORGANIZATION NAME(S) AND ADDRESS(ES) Naval Postgraduate School Monterey, CA 93943-5000			8. PERFORMING ORGANIZATION REPORT NUMBER
9. SPONSORING /MONITORING AGENCY NAME(S) AND ADDRESS(ES) N/A			10. SPONSORING/MONITORING AGENCY REPORT NUMBER
11. SUPPLEMENTARY NOTES The views expressed in this thesis are those of the author and do not reflect the official policy or position of the Department of Defense or the U.S. Government.			
12a. DISTRIBUTION / AVAILABILITY STATEMENT Approved for public release, distribution is unlimited			12b. DISTRIBUTION CODE A

13. ABSTRACT (maximum 200 words)

As the U.S. Navy develops new technologies which enhance automation and reduce crew size onboard naval vessels, unmanned vehicles will become increasingly valuable in conducting maritime operations. Effective launch and recovery systems (LARS) are necessary for unmanned vehicles to efficiently conduct operations at sea. The Towed Body system is a LARS with a wide range of applications for unmanned vehicle operations. The Towed Body can be evaluated as a small vessel with horizontal and vertical control surfaces. Since it is being towed, the directional stability of the Towed Body requires unique consideration due to the presence of the towing force. This thesis examines the effect of varying the longitudinal location of the vertical control surfaces, as well as the effective aspect ratio, size, and number of vertical control surfaces. The results identify critical stability values for the various fin configurations.

14. SUBJECT TERMS Launch and Recovery System (LARS), Unmanned Vehicles (UV), Unmanned Surface Vehicles (USV), Unmanned Underwater Vehicles (UUV), Directional Stability, Motion Stability, Towing Stability			15. NUMBER OF PAGES 81
			16. PRICE CODE
17. SECURITY CLASSIFICATION OF REPORT Unclassified	18. SECURITY CLASSIFICATION OF THIS PAGE Unclassified	19. SECURITY CLASSIFICATION OF ABSTRACT Unclassified	20. LIMITATION OF ABSTRACT UL

NSN 7540-01-280-5500

Standard Form 298 (Rev. 2-89)
Prescribed by ANSI Std. 239-18

THIS PAGE INTENTIONALLY LEFT BLANK

Approved for public release, distribution is unlimited

STABILITY ANALYSIS OF A TOWED BODY FOR SHIPBOARD UNMANNED SURFACE VEHICLE RECOVERY

Scott D. Roberts
Lieutenant, United States Navy
B.S., United States Naval Academy, 1997

Submitted in partial fulfillment of the
requirements for the degree of

MASTER OF SCIENCE IN MECHANICAL ENGINEERING

from the

NAVAL POSTGRADUATE SCHOOL
March 2005

Author: Scott D. Roberts

Approved by: Fotis Papoulias
Thesis Advisor

William Solitario
Second Reader

Anthony J. Healey
Chairman, Department of Mechanical and Astronautical Engineering

THIS PAGE INTENTIONALLY LEFT BLANK

ABSTRACT

As the U.S. Navy develops new technologies which enhance automation and reduce crew size onboard naval vessels, unmanned vehicles will become increasingly valuable in conducting maritime operations. Effective launch and recovery systems (LARS) are necessary for unmanned vehicles to efficiently conduct operations at sea. The Towed Body is a LARS with a wide range of applications for unmanned vehicle operations. The Towed Body can be evaluated as a small vessel with horizontal and vertical control surfaces. Since it is being towed, the directional stability of the Towed Body requires unique consideration due to the presence of the towing force. This thesis examines the effect of varying the longitudinal location of the vertical control surfaces, as well as the effective aspect ratio, size, and number of vertical control surfaces. The results identify critical stability values for the various fin configurations..

THIS PAGE INTENTIONALLY LEFT BLANK

TABLE OF CONTENTS

I. INTRODUCTION 1
A. SHIPBOARD USE OF UNMANNED VEHICLES 1
B. EXISTING METHODS FOR LAUNCH AND RECOVERY 1
C. FUTURE LAUNCH AND RECOVERY SYSTEMS 3
D. TOWED BODY 5

II. EQUATIONS OF MOTION 7
A. EQUATIONS OF MOTION 7
B. YAW AND SWAY SIMPLIFICATION 8
C. CONTROLS FIXED STABILITY 10

III. DEVELOPING HYDRODYNAMIC COEFFICIENTS 13
A. TOWED BODY COMPONENTS 13
1. Body of Revolution 13
2. Vertical Control Surfaces 14
B. TOTAL DERIVATIVES FOR BODY AND FINS 16

IV. TOWING 19
A. GEOMETRY AND NOMENCLATURE 19
B. STABILITY CRITERIA FOR TOWING 20

V. COMPUTER MODELING AND PROBLEM CONFIGURATION 23
A. STABILITY EVALUATION 23
B. VARIABLES 23
1. Number of Fins (n) 23
2. Effective Aspect Ratio (a) 23
3. Longitudinal Location of Fin (x'_F) 23
4. Root Chord Length (C'_{root}) 24
C. MATLAB PROGRAMMING 24

VI. RESULTS 25
A. R_1 STABILITY CRITERIA 25
B. G'_h STABILITY COMPARISON 27
C. R_2 STABILITY CRITERIA 35
1. Impact of n on T'_{crit} 35
2. Impact of a on T'_{crit} 37
a. T'_{crit} *vs.* x'_F *37*
b. T'_{crit} *vs.* C'_{root} *37*
3. Impact of C'_{root} on T'_{crit} 42
4. Impact of x'_F on T'_{crit} 49

VII. CONCLUSIONS AND RECOMMENDATIONS 57

A. CONCLUSIONS 57
B. RECOMMENDATIONS 58
APPENDIX MATLAB PROGRAM FILES 59
A. CALCULATING HYDRODYNAMIC DERIVATIVES 59
1. Body of Revolution Hydrodynamic Derivatives (bodyspec.m) 59
2. Fin Specifications (rudderspec.m) 59
3. Total Hydrodynamic Derivatives for Towed Body (hydroderiv.m) 60
4. Stability Criteria Calculations (stability.m) 60
5. Variable Range Assignment and Data Collection (variables.m) 61
LIST OF REFERENCES 63
INITIAL DISTRIBUTION LIST 65

LIST OF FIGURES

Figure 1. Stern Ramp on USCGC MATAGORDA [http://www.zodiacmilpro.com/product/sbyt/] 2
Figure 2. USS SQUALL (PC 7) with boat handling crane aft 2
Figure 3. AUV A-Frame LARS by Bluefin Robotics[http://www.bluefinrobotics.com/launch.htm] 3
Figure 4. Variable Cradle Concept [SCOUVO] 4
Figure 5. Chinese Lantern UUV Retrieval [SCOUVO] 5
Figure 6. Towed Body Concept [SCOUVO] 6
Figure 7. Coordinate Frames on USS SQUALL (PC 7) [after USS SQUALL command photograph] 7
Figure 8. Rudder-induced turning moments [PNA] 9
Figure 9. Motion stability [PNA] 10
Figure 10. Approximate Suboff Body [Wolkerstorfer] 13
Figure 11. NACA 0015 Rudder Cross Section [PNA] 14
Figure 12. Specifications and Terminology for an all-movable rudder [PNA] 15
Figure 13. Towing Geometry [Bernitsas] 19
Figure 14. Towed Body 24
Figure 15. G'_h values for a=0.5 and 1.0 29
Figure 16. G'_h values for a=1.5 and 2.0 30
Figure 17. G'_h values for a=2.5 and 3.0 31
Figure 18. G'_h values for a=3.5 and 4.0 32
Figure 19. G'_h values for a=4.5 and 5.0 33
Figure 20. G'_h values for a=5.5 and 6.0 34
Figure 21. Effect of n on T'_{crit} for a = 1 to 4 36
Figure 22. Effect of a on T'_{crit} for specified C'_{root} values, n = 1 38
Figure 23. Effect of a on T'_{crit} for specified C'_{root} values, n = 2 39
Figure 24. Effect of a on T'_{crit} for specified x'_F values, n = 1 40
Figure 25. Effect of a on T'_{crit} for specified x'_F values, n = 2 41
Figure 26. Effect of C'_{root} on T'_{crit} for a = 0.5 and 1.0 43
Figure 27. Effect of C'_{root} on T'_{crit} for a = 1.5 and 2.0 44
Figure 28. Effect of C'_{root} on T'_{crit} for a = 2.5 and 3.0 45
Figure 29. Effect of C'_{root} on T'_{crit} for a = 3.5 and 4.0 46
Figure 30. Effect of C'_{root} on T'_{crit} for a = 4.5 and 5.0 47
Figure 31. Effect of C'_{root} on T'_{crit} for a = 5.5 and 6.0 48
Figure 32. Effect of x'_F on T'_{crit} for a = 0.5 and 1.0 50

Figure 33. Effect of x'_F on T'_{crit} for a = 1.5 and 2.0.....51
Figure 34. Effect of x'_F on T'_{crit} for a = 2.5 and 3.0.....52
Figure 35. Effect of x'_F on T'_{crit} for a = 3.5 and 4.0.....53
Figure 36. Effect of x'_F on T'_{crit} for a = 4.5 and 5.0.....54
Figure 37. Effect of x'_F on T'_{crit} for a = 5.5 and 6.0.....55

LIST OF TABLES

Table 1. SUBOFF Hydrodynamic Coefficients 14
Table 2. SUBOFF values interpolated from DSRV data 14
Table 3. Critical Values for R_1 Stability Criteria 26
Table 4. R_1 and G_h' Comparison for a=1, C'_{root} =0.08 27

THIS PAGE INTENTIONALLY LEFT BLANK

ACKNOWLEDGMENTS

I would like to thank Mr. F. Mark Mulhern for providing valuable information on the design history of the Towed Body and details on its operational employment. Thanks are also in order to Professor William Solitario for providing the opportunity to discuss unmanned vehicle launch and recovery systems with industry experts. Finally, the excellent assistance I received from Professor Fotis Papoulias provided the necessary technical guidance to develop the MATLAB codes and properly analyze the results developed in this thesis. The completion of this work would not have been possible without the support of my wife and children.

THIS PAGE INTENTIONALLY LEFT BLANK

I. INTRODUCTION

A. SHIPBOARD USE OF UNMANNED VEHICLES

As the U.S. Navy develops new technologies which enhance automation and reduce crew size onboard naval vessels, unmanned vehicles will become increasingly valuable in conducting maritime operations. These vehicles will be capable of performing a variety of missions such as surface search, force protection, maritime interdiction, and mine warfare.

In order to effectively employ unmanned vehicles from onboard ship, efficient handling systems are necessary for the launch and recovery of these vehicles. The process of launching and recovering unmanned surface vehicles (USV) and unmanned underwater vehicles (UUV) can be a difficult and labor intensive evolution under adverse conditions. High winds and high sea states produce unfavorable relative motions between the unmanned vehicle and ship, increasing the risk of damage and personnel injury.

B. EXISTING METHODS FOR LAUNCH AND RECOVERY

The process of launching and recovering a small boat from a ship is a common procedure. Current naval vessels utilize boat davits in order to accomplish this task. This system requires numerous crew members to operate the davit and hold steadying lines while the boat is raised or lowered into the water. Under ideal conditions, this is a relatively safe and easy evolution. High winds and sea states cause a significant increase in the relative motion between the ship and small boat, which in turn increases the threat of damage to the vessels and for personnel injury.

Some smaller U.S. naval vessels and U.S. Coast Guard vessels utilize a stern ramp for launch and recovery of small boats. This method of launch and recovery makes it possible to conduct the evolution with fewer personnel, but the risk of damage in higher sea states still exists due to the relative motion between the boat and the ship. Also, the added effect of operating directly in the wake of the ship must be considered for the performance of the small boat attempting to maneuver into the stern ramp. Overall, as

compared to the boat davit, the stern ramp provides a safer and more effective method for launch and recovery of small boats. [Sheinberg, Cleary, Beukema]

Figure 1. Stern Ramp on USCGC MATAGORDA
[http://www.zodiacmilpro.com/product/sbyt/]

Originally constructed as a 110 foot Island class Patrol Boat, figure (1) shows the USCGC MATAGORDA after completing a service life extension program (SLEP). This overhaul lengthened the ship to 123 feet and replaced a boat handling crane with a stern ramp [Gourley]. Several U.S. Navy Cyclone class Patrol Craft received similar overhauls where the boat handling crane was removed and replaced with a stern ramp for small boat launch and recovery.

Figure 2. USS SQUALL (PC 7) with boat handling crane aft

Cranes are utilized by some naval vessels and commercial vessels for launching and recovering small boats and underwater vehicles. Oceanographic research vessels use cranes or A-Frames to handle various types of underwater vehicles. Existing crane systems require personnel to operate the crane and handle steadying lines to the vehicle.

High winds and high sea states again cause large relative motions between the ship and the vehicle. This makes the process of connecting the vehicle to the crane cable difficult to accomplish as a result of the magnitude of the ship and vehicle motions.

Figure 3. AUV A-Frame LARS by Bluefin Robotics[http://www.bluefinrobotics.com/launch.htm]

C. FUTURE LAUNCH AND RECOVERY SYSTEMS

The Innovation Center at Naval Surface Warfare Center, Carderock Division published a report in 2003 assessing new concepts for unmanned vehicle launch and recovery. This study, titled SCOUVO (Surface Combatant Optimized for Unmanned Vehicle Operations) evaluated three different hull forms along with several launch, recovery, and onboard handling systems optimized for use with unmanned vehicles. For launch and recovery, the study examined five systems: an automated crane system (Homing Crane), Variable Geometry Cradle, Towed Body, Paravane, and Chinese Lantern.

The Homing Crane allows for reduced manning when operating the system and provides a soft initial connection between the ship and unmanned vehicle. The crane is motion controlled and maneuvers itself to pick up the vehicle alongside the ship. This can be used for both USV and UUV operations.

The Variable Cradle is utilized with a stern ramp. The cradle changes the geometry of the landing area to provide proper support for the particular UV which it will hold. This allows the cradle to hold a variety of vehicles with varying hull forms. This system is also USV and UUV capable.

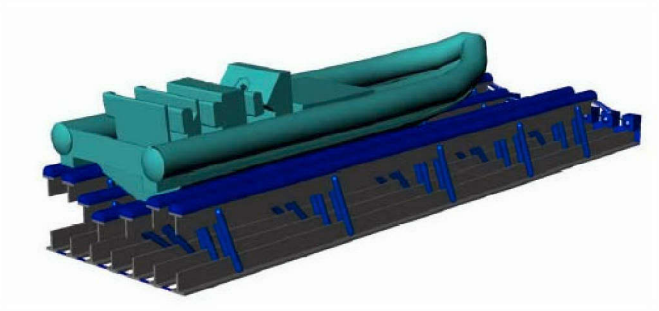

Figure 4. Variable Cradle Concept [SCOUVO]

The Towed Body is a maneuverable body which is towed astern of the launch and recovery ship. It allows for a soft connection between the ship and UV and can be complemented with a crane or stern ramp. This system will operate with both USVs and UUVs.

The Paravane is also towed behind the ship and snares the UV. This concept is based on the A/N37U-1 Mine Clearing Set.

Only for use with UUVs, the Chinese Lantern can retrieve multiple vehicles at once. This system drags a line behind the ship with several hook-up locations along the length of the line. The UUVs maneuver to the hook-up points on the line, and the ship retrieves the vehicles when desired [SCOUVO].

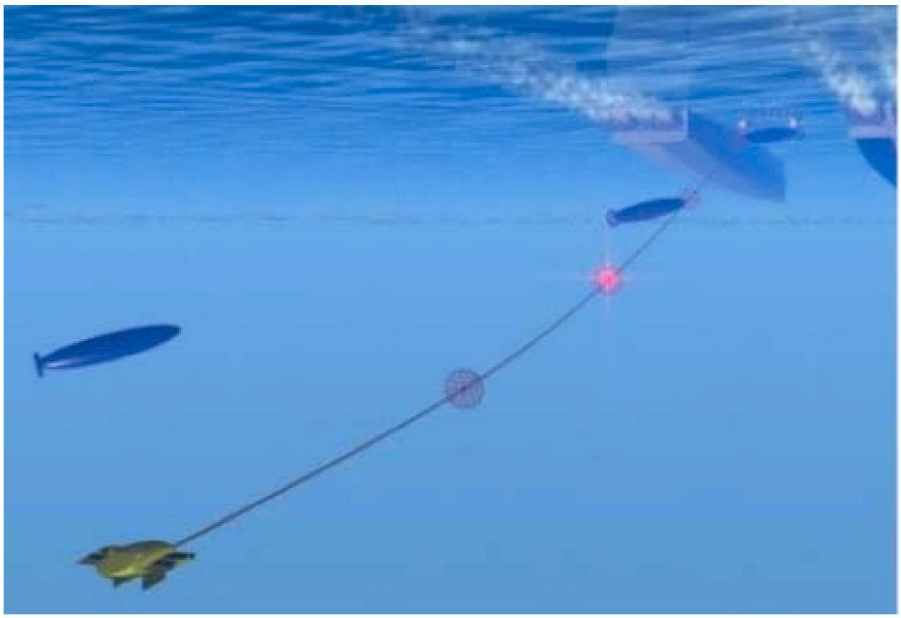

Figure 5. Chinese Lantern UUV Retrieval [SCOUVO]

D. TOWED BODY

This thesis will examine the directional stability of the Towed Body launch and recovery system. Since this concept has the potential to function with a wide variety of vehicles and may be used with a stern ramp or crane, it is a possible launch and recovery solution with many applications.

The concept for the Towed Body was initially developed late in the Cold War for underway refueling of surface combatants. The body would be located at the end of a refueling line and allow for a low signature underway refueling evolution by eliminating the need for standard topside refueling rigging [Mulhern].

The Towed Body concept was reintroduced as a UV launch and recovery system in the SCOUVO report. In addition to enabling a soft connection between the UV and ship for retrieval, the towline can also carry with it a means to refuel the vehicle or provide a connection for data to be passed between the UV and ship. This allows for multiple sorties of the UV without needing to recover the vehicle onboard ship each time.

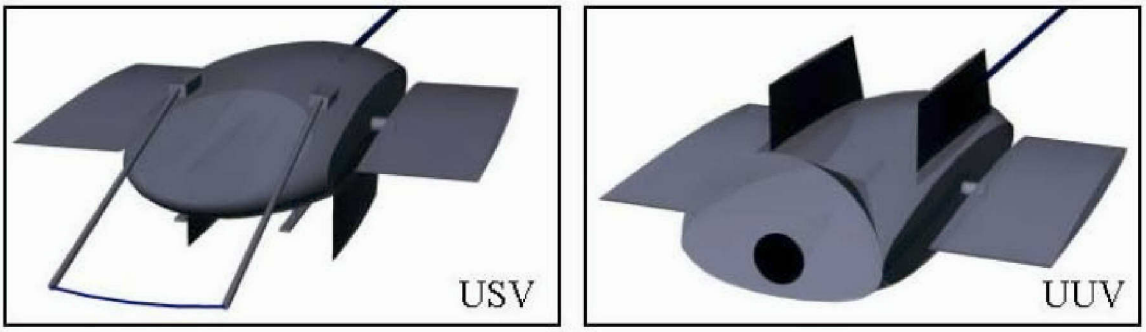

Figure 6. Towed Body Concept [SCOUVO]

The conceptual design of the towed body has a wingspan of approximately three feet and a body length of about five feet. The control surfaces (wings and fins) are moved by electrically driven actuators. The fins are located on the bottom of the body to allow the hook-up device for grasping the UV to be located on top of the body.

The retrieval capacity of the Towed Body system depends primarily on the size of the tow cable and the capacity of the constant tension winch used to reel in the tow cable. The system is envisioned to accommodate any UV up to 20,000 pounds, approximately the size of a U.S. Navy 11 meter RHIB.

To accomplish the hook up between the Towed Body and the UV, the Towed Body will be equipped with a guidance system similar to that of a heat seeking missile. The UV will carry an optical emitter for the towed body to locate and then maneuver to that location. This is an experimental guidance system that has not been tested in an operational environment [Mulhern]. The harness on the Towed Body used to connect to the UV operates like a mousetrap. Once the UV trips the harness, the Towed Body is reeled in back to the ship. The vertical fins on the towed body are able to retract in order to allow the body and the UV to be pulled onto a stern ramp without damage.

The Towed Body design differs slightly for USV and UUV use, as seen in Figure 6. This study will focus only on USV operations. The Towed Body is assumed to be operating in the vicinity of the ocean surface and will only maneuver in the x-y plane. No change in depth will occur. This assumption permits the wings to be ignored and as such will not be included in the model developed in this thesis.

II. EQUATIONS OF MOTION

A. EQUATIONS OF MOTION

A marine vehicle has six degrees of freedom in which it can move when operating without any restraints. Figure 7 shows the three translational degrees of freedom (surge, sway, and heave) and the three rotational degrees of freedom (pitch, roll, and yaw) on and about the x, y, and z axes.

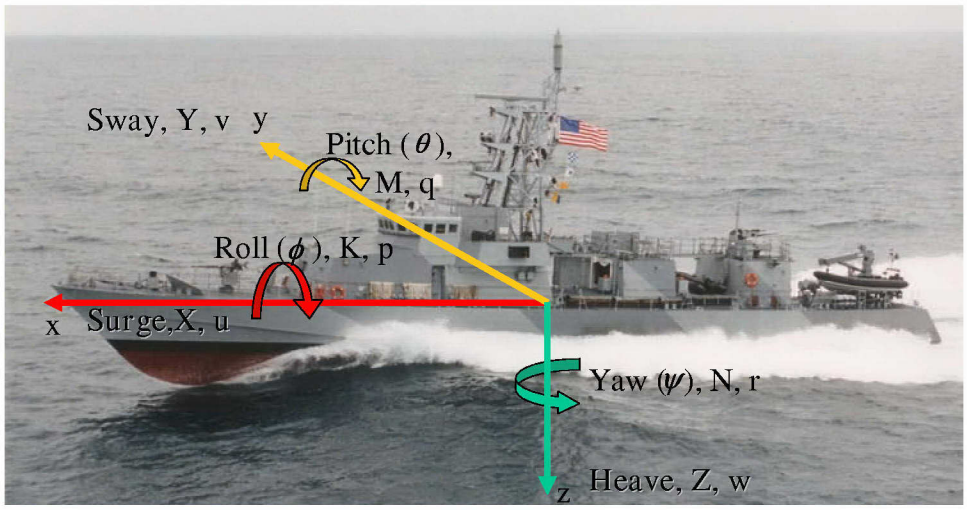

Figure 7. Coordinate Frames on USS SQUALL (PC 7) [after USS SQUALL command photograph]

The equations of motion for all six degrees freedom, as derived in [Healey (2001)] are:

$$
\begin{aligned}
&SURGE: && m\left[\dot{u}-vr+wq-x_G\left(q^2+r^2\right)+y_G\left(pq-\dot{r}\right)+z_G\left(pr+\dot{q}\right)\right]=X\\
&SWAY: && m\left[\dot{v}+ur-wp+x_G\left(pq+\dot{r}\right)-y_G\left(p^2+r^2\right)+z_G\left(qr-\dot{p}\right)\right]=Y\\
&HEAVE: && m\left[\dot{w}-uq+vp+x_G\left(pr-\dot{q}\right)+y_G\left(qr+\dot{p}\right)-z_G\left(p^2+q^2\right)\right]=Z\\
&ROLL: && I_x\dot{p}+\left(I_z-I_y\right)qr+I_{xy}\left(pr-\dot{q}\right)-I_{yz}\left(q^2-r^2\right)-I_{xz}\left(pq+\dot{r}\right)\\
& && \quad +m\left[y_G\left(\dot{w}-uq+vp\right)-z_G\left(\dot{v}+ur-wp\right)\right]=K \qquad (2.1)\\
&PITCH: && I_y\dot{q}+\left(I_x-I_z\right)pr-I_{xy}\left(qr+\dot{p}\right)+I_{yz}\left(pq-\dot{r}\right)+I_{xz}\left(p^2-r^2\right)\\
& && \quad -m\left[x_G\left(\dot{w}-uq+vp\right)-z_G\left(\dot{u}-vr+wq\right)\right]=M\\
&YAW: && I_z\dot{r}+\left(I_y-I_x\right)pq-I_{xy}\left(p^2-q^2\right)-I_{yz}\left(pr+\dot{q}\right)+I_{xz}\left(qr-\dot{p}\right)\\
& && \quad +m\left[x_G\left(\dot{v}+ur-wp\right)-y_G\left(\dot{u}-vr+wq\right)\right]=N
\end{aligned}
$$

B. YAW AND SWAY SIMPLIFICATION

The analysis in this thesis is focused on the directional stability of the towed body for USV operations, so several simplifications can be made to reduce the equations of motion. First, any environmental forces that may act on the towed body, such as wind and waves, will be ignored. For USV retrieval, the towed body will operate in the vicinity of the ocean surface and will not perform any depth changes. Also, it is assumed that the towed body will be subjected to a constant towing force and that it will have the same forward velocity as the towing vessel. These assumptions allow the equations of motion to be reduced down to the two equations for sway and yaw. Surge, heave, pitch, and roll are neglected in this study.

Following the justification and simplified derivative notation of the Society of Naval Architects and Marine Engineers (SNAME) [PNA], the equations of motion are reduced as follows:

$$
\begin{aligned}
&SWAY: -Y_v v+\left(m-Y_{\dot{v}}\right)\dot{v}-\left(Y_r-mU\right)r-Y_{\dot{r}}\dot{r}=0\\
&YAW: -N_v v-N_{\dot{v}}\dot{v}-N_r r+\left(I_z-N_{\dot{r}}\right)\dot{r}=0
\end{aligned}
\qquad (2.2)
$$

The terms $Y_v v$ and $Y_r r$ represent the lateral force due to side slip velocity and yaw rate respectively. The terms $N_v v$ and $N_r r$ represent the moment caused by side slip velocity and yaw rate. The term m represents the mass of the vessel, U is the forward velocity, and I_z is the mass moment of inertia about the z axis.

These equations are nondimensionalized in order to permit easier use of available data. Nondimensional terms are denoted with a prime superscript. The sway equation consists of force terms and is nondimensionalized by dividing with $(\rho/2)L^2V^2$. The yaw equation consists of moment terms and is nondimensionalized by dividing with $(\rho/2)L^3V^2$. This yields:

$$\begin{aligned} SWAY &: -Y_v'v' + \left(m' - Y_{\dot{v}}'\right)\dot{v}' - \left(Y_r' - m'\right)r' - Y_{\dot{r}}'\dot{r}' = 0 \\ YAW &: -N_v'v' - N_{\dot{v}}'\dot{v}' - N_r'r' + \left(I_z' - N_{\dot{r}}'\right)\dot{r}' = 0 \end{aligned} \tag{2.3}$$

Forward velocity, U, is nondimensionalized with ship's speed, so $u'=1$ and the term is dropped from the equation.

Additional sway forces and yaw moments are produced by the deflection of a vertical control surface, such as a rudder. Figure 8 shows the turning moments produced by rudder deflection on a ship.

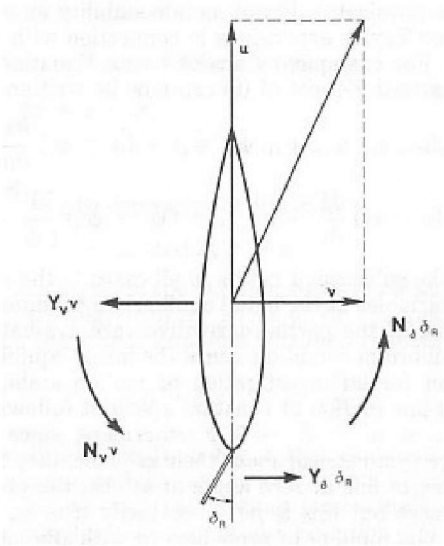

Figure 8. Rudder-induced turning moments [PNA]

The rudder deflection angle is identified by δ_R, and Y_δ and N_δ are the derivatives of Y and N with respect to the rudder deflection angle. These terms may also be nondimensionalized, and are included in the sway and yaw expressions as follows:

$$SWAY: -Y_v'v' + \left(m' - Y_{\dot{v}}'\right)\dot{v}' - \left(Y_r'm'\right)r' - Y_{\dot{r}}'\dot{r}' = Y_\delta'\delta_R$$
$$YAW: -N_v'v' - N_{\dot{v}}'\dot{v}' - N_r'r' + \left(I_z' - N_{\dot{r}}'\right)\dot{r}' = N_\delta'\delta_R \tag{2.4}$$

For the purpose of this study, the forces and moments produced by the rudder will be considered, but only with the rudder held at zero degrees.

C. CONTROLS FIXED STABILITY

When a vessel is moving in a straight line path and encounters an instantaneous disturbance, the subsequent path of the vessel illustrates its motion stability. If the vessel resumes a straight line path, regardless of direction after the disturbance occurs, it is considered to have straight line stability. A vessel with directional stability is able to resume the straight line path in the same direction as the original path. Figure 9 illustrates the different types of motion stability.

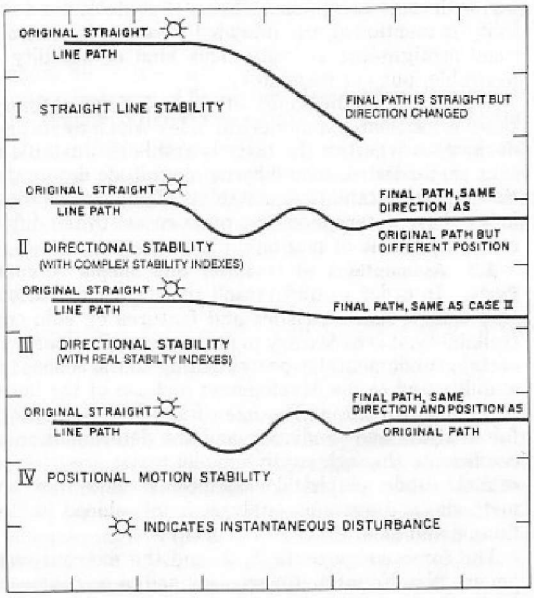

Figure 9. Motion stability [PNA]

The straight line stability of a vessel can be determined with the characteristic equation:

$$A\sigma^2 + B\sigma + C = 0 \tag{2.5}$$

where

$$
\begin{aligned}
A &= \left(I'_z - N'_{\dot{r}}\right)\left(m' - Y'_{\dot{v}}\right) - \left(Y'_{\dot{r}} - m'x'_G\right)\left(N'_{\dot{v}} - m'x'_G\right) \\
B &= -\left(I'_z - N'_{\dot{r}}\right)Y'_v - \left(m' - Y'_{\dot{v}}\right)\left(N'_r - m'x'_G u'\right) \\
&\quad - \left(Y'_r - m'u'\right)\left(N'_{\dot{v}} - m'x'_G\right) - \left(Y'_{\dot{r}} - m'x'_G\right)N'_v \\
C &= \left(N'_r - m'x'_G u'\right)Y'_v - \left(Y'_r - m'u'\right)N'_v
\end{aligned}
\tag{2.6}
$$

In order to meet the stability criteria, A, B, and C must be greater than zero. The value of C is termed the stability index. Generally, a positive stability index indicates that the ship is stable. Alternatively, the stability index can be found in normalized manner with the expression:

$$
G_h = 1 - \frac{N'_v\left(Y'_r - m'\right)}{Y'_v\left(N'_r - m'x'_G\right)} \tag{2.7}
$$

Equation 2.7 allows for easier comparison and plotting of the stability index [Papoulias].

THIS PAGE INTENTIONALLY LEFT BLANK

III. DEVELOPING HYDRODYNAMIC COEFFICIENTS

A. TOWED BODY COMPONENTS

The Towed Body LARS is currently a conceptual design, so there are no existing models or specifications available for evaluating the directional stability of the design. In order to develop a model for the purpose of this thesis, existing data for similar body shapes were utilized in a nondimensional format.

1. Body of Revolution

The geometry of the towed body can be modeled with an existing body of revolution, the Defense Advanced Research Projects Agency (DARPA) SUBOFF model, developed at the Naval Surface Warfare Center, Carderock Division (NSWCCD). This model was utilized by [Wolkerstorfer] in his work with SLICE pods. Wolkerstorfer approximated the SUBOFF body as a body of revolution with an elliptical nose, cylindrical mid body, and a conical base section.

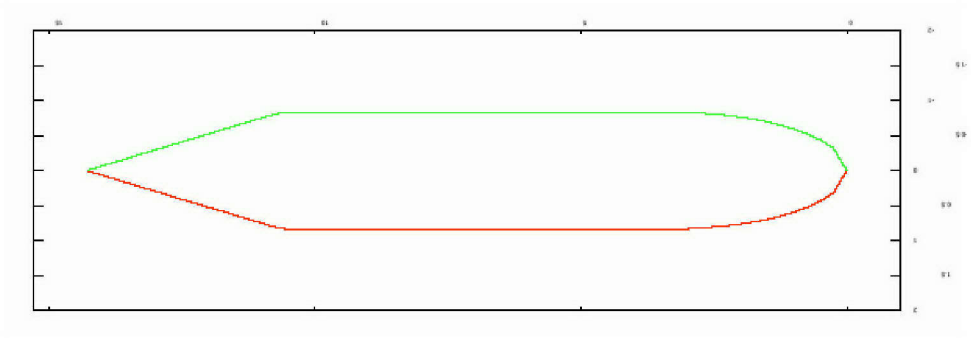

Figure 10. Approximate Suboff Body [Wolkerstorfer]

The nondimensional hydrodynamic coefficients for the SUBOFF body were determined through captive model tests at NSWCCD. These values, shown in Table 1 are used in this study of the Towed Body.

Y'_v	-0.005948	$Y'_{\dot{v}}$	-0.013278
Y_r	0.001811	$Y'_{\dot{r}}$	0.000060
N'_v	-0.012795	$N'_{\dot{v}}$	0.000202
N'_r	-0.001597	$N'_{\dot{r}}$	-0.000676

Table 1. SUBOFF Hydrodynamic Coefficients

Nondimensional values for mass and mass moment of inertia were not available for the approximate SUBOFF body. For an acceptable approximation of these values, the coefficients from the U.S. Navy DSRV were used to establish a linear relation between mass and $Y'_{\dot{v}}$ and between I'_z and $N'_{\dot{r}}$. This relation was then applied to the $Y'_{\dot{v}}$ and $N'_{\dot{r}}$ values for the SUBOFF body to obtain acceptable values for m' and I'_z. [*DSRV*]

m'	0.013594
I'_z	0.00084997

Table 2. SUBOFF values interpolated from DSRV data

2. Vertical Control Surfaces

The fins for the Towed Body are modeled using the standard NACA 0015 geometry as an all-movable rudder. This rudder design has a square tip shape, taper ratio of 0.45, sweep angle of zero, and a thickness to chord ratio of 0.15. This standard geometry scales easily with various aspect ratios and chord lengths.

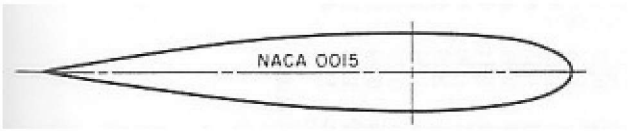

Figure 11. NACA 0015 Rudder Cross Section [PNA]

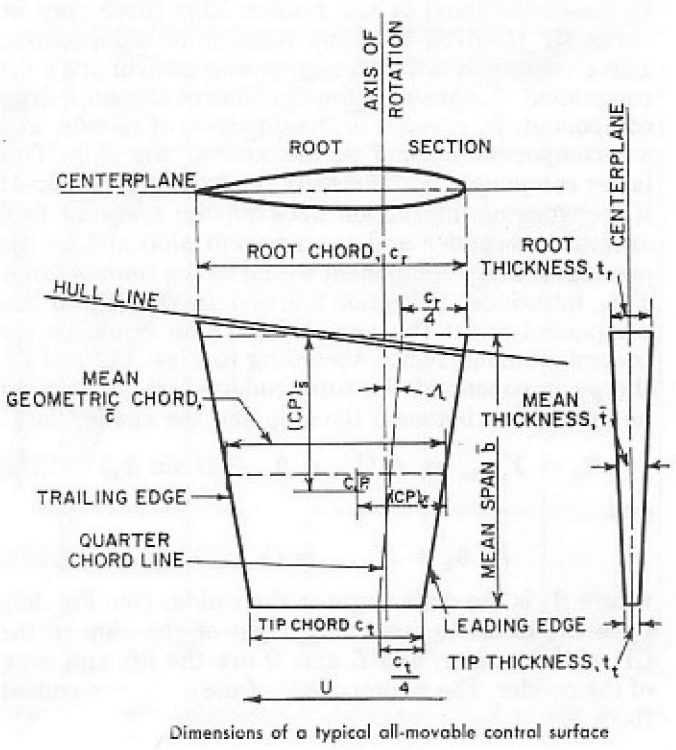

Figure 12. Specifications and Terminology for an all-movable rudder [PNA]

The geometric aspect ratio is determined by dividing the mean span by the mean chord length. The effective aspect ratio takes into consideration the groundboard effect of the fin being mounted to a flat surface. For the towed body, a groundboard condition is assumed, so the effective ratio is two times the geometric aspect ratio [PNA].

The longitudinal location of the rudder is described with the variable x_F, the longitudinal distance from the center of the body of revolution to the center of the rudder. Positive values of x_F indicate that the rudder is located forward of amidships, or the center of the Towed Body.

Experimental data provides the most accurate method of determining hydrodynamic coefficients. Since experimentation is not always practical, theoretical calculation is acceptable. The theoretical calculations in this study determine the hydrodynamic coefficients of the fixed vertical control fins within a linear range. Following the theoretical development in Principles of Naval Architecture, Volume III, the hydrodynamic coefficients for a fixed fin are expressed:

$$
\begin{aligned}
\left(Y'_v\right)_f &= -\left|A'_f\left(\frac{\partial C_L}{\partial \beta}\right)_f\right| \\
\left(N'_v\right)_f &= \left(Y'_v\right)_f x'_f \\
\left(Y'_r\right)_f &= \left(Y'_v\right)_f x'_f \\
\left(N'_r\right)_f &= \left(Y'_v\right)_f x'^2{}_f \\
\left(Y'_{\dot{v}}\right)_f &= -\frac{2\pi b' A'_f}{\sqrt{a_G^2+1}} \\
\left(N'_{\dot{v}}\right)_f &= \left(Y'_{\dot{v}}\right)_f x'_f \\
\left(Y'_{\dot{r}}\right)_f &= \left(Y'_{\dot{v}}\right)_f x'_f \\
\left(N'_{\dot{r}}\right)_f &= \left(Y'_{\dot{v}}\right)_f x'^2{}_f
\end{aligned}
\qquad (3.1),
$$

A_f = area of fin

b = geometric span (3.2)

$a_G = b^2 / A_f$

Using Jone's Formula for low aspect ratio fins, $\frac{\partial C_L}{\partial \beta} = \left(\frac{\pi}{2}\right)a$, where a is the effective aspect ratio of the fin. Since the groundboard condition is assumed for the towed body design, $a = 2a_G$. These relations reduce $\left(Y'_v\right)_f$ and $\left(Y'_{\dot{v}}\right)_f$ from equation 3.1 to:

$$
\begin{aligned}
\left(Y'_v\right)_f &= -\left|A'_f\left(\frac{\pi}{2}\right)a\right| \\
\left(Y'_{\dot{v}}\right)_f &= -\frac{4\pi b' A'_f}{\sqrt{a^2+1}}
\end{aligned}
\qquad (3.3)
$$

B. TOTAL DERIVATIVES FOR BODY AND FINS

In order to develop the hydrodynamic coefficients for the towed body including the fins, the individual derivatives for the body and each appendage are summed. For a towed body design using only one vertical fin, the hydrodynamic coefficients would be:

$$
\begin{aligned}
Y'_v &= \left(Y'_v\right)_h + \left(Y'_v\right)_f \\
N'_v &= \left(N'_v\right)_h + \left(N'_v\right)_f \\
Y'_r &= \left(Y'_r\right)_h + \left(Y'_r\right)_f \\
N'_r &= \left(N'_r\right)_h + \left(N'_r\right)_f \\
Y'_{\dot{v}} &= \left(Y'_{\dot{v}}\right)_h + \left(Y'_{\dot{v}}\right)_f \\
N'_{\dot{v}} &= \left(N'_{\dot{v}}\right)_h + \left(N'_{\dot{v}}\right)_f \\
Y'_{\dot{r}} &= \left(Y'_{\dot{r}}\right)_h + \left(Y'_{\dot{r}}\right)_f \\
N'_{\dot{r}} &= \left(N'_{\dot{r}}\right)_h + \left(N'_{\dot{r}}\right)_f
\end{aligned}
\tag{3.4}
$$

When two fins are evaluated in this study, both fins are assumed to be at the same longitudinal location on the body, and equally offset from centerline. From equation 3.4, this yields:

$$
\begin{aligned}
Y'_v &= \left(Y'_v\right)_h + 2\left(Y'_v\right)_f \\
N'_v &= \left(N'_v\right)_h + 2\left(N'_v\right)_f \\
Y'_r &= \left(Y'_r\right)_h + 2\left(Y'_r\right)_f \\
N'_r &= \left(N'_r\right)_h + 2\left(N'_r\right)_f \\
Y'_{\dot{v}} &= \left(Y'_{\dot{v}}\right)_h + 2\left(Y'_{\dot{v}}\right)_f \\
N'_{\dot{v}} &= \left(N'_{\dot{v}}\right)_h + 2\left(N'_{\dot{v}}\right)_f \\
Y'_{\dot{r}} &= \left(Y'_{\dot{r}}\right)_h + 2\left(Y'_{\dot{r}}\right)_f \\
N'_{\dot{r}} &= \left(N'_{\dot{r}}\right)_h + 2\left(N'_{\dot{r}}\right)_f
\end{aligned}
\tag{3.5}
$$

THIS PAGE INTENTIONALLY LEFT BLANK

IV. TOWING

A. GEOMETRY AND NOMENCLATURE

The towed body must be evaluated in a slightly different manner than a free maneuvering ship due to the presence of the tow cable force. It is assumed that the hydrodynamic coefficients are determined in the same fashion as previously described, but the stability criterion takes into account the impact of the towing force.

Figure 13 illustrates the geometry and terms for developing the equations of motion for a towed vessel.

u_0 = towing vessel's forward velocity
l = length of the unstrained towline
T = tension of the towline
L = length of the towed body
x_p = distance from towed body's CG to tow connection
y_o = towed body's offset from towing ship's line of motion
ψ = towed body yaw angle
x = distance between two vessels in x direction

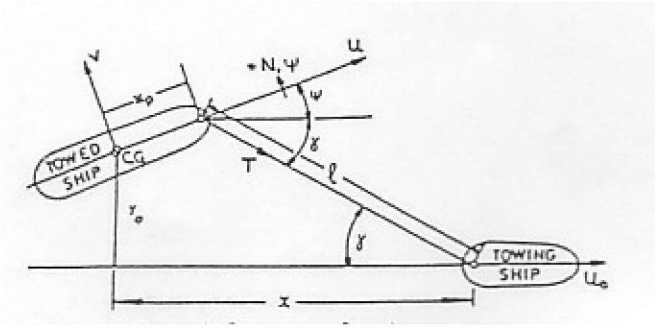

Figure 13. Towing Geometry [Bernitsas]

The addition of the tow cable force alters the relevant nondimensional equations of motion in equation 2.3 as follows [Latorre]:

$$
\begin{aligned}
SWAY:\ & \left(Y'_{\dot v}-m'\right)\ddot y'_0+Y'_v\dot y'_0-\frac{T'}{l'}y_0+Y'_{\dot r}\ddot\psi'-\left(Y'_v u'-Y'_r\right)\dot\psi' \\
& \qquad -\left(Y'_v u'+T'\left(1+\frac{x'_p}{l'}\right)+\left(Y'_{\dot v}-m'\right)\dot u'\right)\psi'=0 \\
YAW:\ & N_{\dot v}\ddot y_0+N_v\dot y_0-\frac{T'}{l'}x'_p y'_0+\left(N'_{\dot r}-I'_z\right)\ddot\psi-\left(N'_{\dot v}u'-N'_r\right)\dot\psi' \\
& \qquad -\left(N'_v u'+T'x'_p\left(1+\frac{x'_p}{l'}\right)+N'_{\dot v}\dot u'\right)\psi'=0
\end{aligned}
\tag{4.1}
$$

B. STABILITY CRITERIA FOR TOWING

The characteristic equation used for evaluating the stability of a towed vessel, as derived in [Latorre] and [Bernitsas] is of the form:

$$A\sigma^4+B\sigma^3+C\sigma^2+D\sigma+E=0 \tag{4.2}$$

Where

$$
\begin{aligned}
A&=\left(Y'_{\dot v}-m'\right)\left(N'_{\dot r}-I'_z\right)-N'_{\dot v}Y'_{\dot r} \\
B&=\left(Y'_{\dot v}-m'\right)\left(N'_r-N'_{\dot v}u'\right)+Y'_v\left(N'_{\dot r}-I'_z\right)+\left(Y'_{\dot v}u'-Y'_r\right)N'_{\dot v}-Y'_{\dot r}N'_v \\
C&=Y'_v\left(N'_r-N'_{\dot v}u'\right)-\frac{T'}{l'}\left(N'_{\dot r}-I'_z\right)+\left(Y'_{\dot v}-m'\right)\left[-N'_v u'-T'x'_p\left(1+\frac{x'_p}{l'}\right)\right]+\left(Y'_{\dot v}u'-Y'_r\right)N'_v+Y'_{\dot r}\left(\frac{T'x'_p}{l'}\right) \\
D&=Y'_v\left[-N'_v u'-T'x'_p\left(1+\frac{x'_p}{l'}\right)\right]+\frac{T'}{l'}\left(N'_{\dot v}u'-N'_r\right)-\left(Y'_{\dot v}u'-Y'_r\right)\frac{T'x'_p}{l'}+N'_v\left[Y'_v u'+T'\left(1+\frac{x'_p}{l'}\right)\right] \\
E&=\frac{T'}{l'}\left[N'_v u'+T'x'_p\left(1+\frac{x'_p}{l'}\right)\right]-\left[Y'_v u'+T'\left(1+\frac{x'_p}{l'}\right)\right]T'\frac{x'_p}{l'}
\end{aligned}
\tag{4.3}
$$

Towing is determined to be stable if all real parts of the roots of the characteristic equation are negative. The work of [Latorre] and [Bernitsas] further show that B, D, E, and $BCD-AD^2-B^2E$ must all be greater than zero. Also, since T, l, and x_p are the most important parameters in towing, the terms in A, B, C, D, and E may be organized with subscript '0' for terms in the maneuvering stability criteria, '1' for coefficients of T, and '2' for coefficients of T/l. This results in:

$$
\begin{aligned}
A &= A_0 \\
B &= B_0 \\
C &= C_0 + T'\left[C_1 + \frac{C_2}{l'}\right] \\
C_0 &= Y_v' N_r' + N_v'\left(m' - Y_r'\right) \\
C_1 &= \left(m' - Y_{\dot{v}}'\right) x_p' + N_{\dot{v}}' \\
C_2 &= -\left(N_{\dot{r}}' - I_z'\right) + \left(m' - Y_{\dot{v}}'\right) x_p'^2 + x_p'\left(N_{\dot{v}}' + Y_{\dot{r}}'\right) \\
D &= T'\left[D_1 + \frac{D_2}{l'}\right] \\
D_1 &= N_v' - Y_v' x_p' \\
D_2 &= -Y_v' x_p'^2 + N_v' x_p' + \left(Y_r' - Y_{\dot{v}}'\right) x_p' - N_r' + N_{\dot{v}}' \\
E &= \frac{T'}{l'} E_2 \\
E_2 &= D_1
\end{aligned}
\tag{4.4}
$$

Ultimately, there are two active criteria for ship towing stability. The first criteria, R_1, is determined by the following inequality:

$$
R_1: \; x_p' > \frac{N_v'}{Y_v'} \tag{4.5}
$$

The second criteria, R_2, is determined by the inequality

$$
R_2: \; T' > -\alpha_2 / \alpha_1 \tag{4.6}
$$

where

$$
\begin{aligned}
\alpha_1 &= \left(B_0 C_1 D_1 - A_0 D_1^2\right) + \frac{1}{l'}\left(B_0 C_1 D_2 + B_0 C_2 D_1 - 2 A_0 D_1 D_2\right) + \frac{1}{l'^2}\left(B_0 C_2 D_2 - A_0 D_2^2\right) \\
\alpha_2 &= B_0 C_0 D_1 + \frac{1}{l'}\left(B_0 C_0 D_2 - B_0^2 E_2\right)
\end{aligned}
\tag{4.7}
$$

The inequality in R_2 can also be used to identify the critical value for T' which makes towing stable because the values α_1 and α_2 are independent of speed, resistance, and tow cable tension.

THIS PAGE INTENTIONALLY LEFT BLANK

V. COMPUTER MODELING AND PROBLEM CONFIGURATION

A. STABILITY EVALUATION

The calculations conducted in this thesis will determine if the R_1 stability criteria is satisfied for a range of fin sizes, effective aspect ratios, and longitudinal locations on the towed body. Also, the critical value for T', the nondimensional tow cable tension, will be identified for the various fin configurations.

B. VARIABLES

The four variables used to find the stability characteristics for a wide range of fin configurations are: Number of fins (n), effective aspect ratio (a), nondimensional longitudinal location of the fin (x'_F), and the nondimensional root chord length of the fin (C'_{root}).

1. Number of Fins (n)

Calculations are conducted for a Towed Body with no vertical control surfaces, one, and two vertical control surfaces. When one fin is used, it is located on the centerline of the body. For the case of two vertical control surfaces, the fins are located at the same longitudinal location on the body, and are placed symmetrically about the centerline of the body.

2. Effective Aspect Ratio (a)

The effective aspect ratio is two times the geometric aspect ratio following the groundboard assumption previously discussed. Calculations are conducted for effective aspect ratios ranging from 0.5 to 6.0 at an interval of 0.5.

3. Longitudinal Location of Fin (x'_F)

The nondimesnional value x'_F is found by dividing x_F by the vessel length. The fins will be evaluated at locations ranging from amidships to the stern. As a rudder is moved forward on a ship, it becomes less effective. A Towed Body configuration with fins forward of amidships is not sensible due to this and the presence of the towing force near the bow. Therefore, the values for x'_F will range from -0.04 to -0.5 at an interval of -0.02.

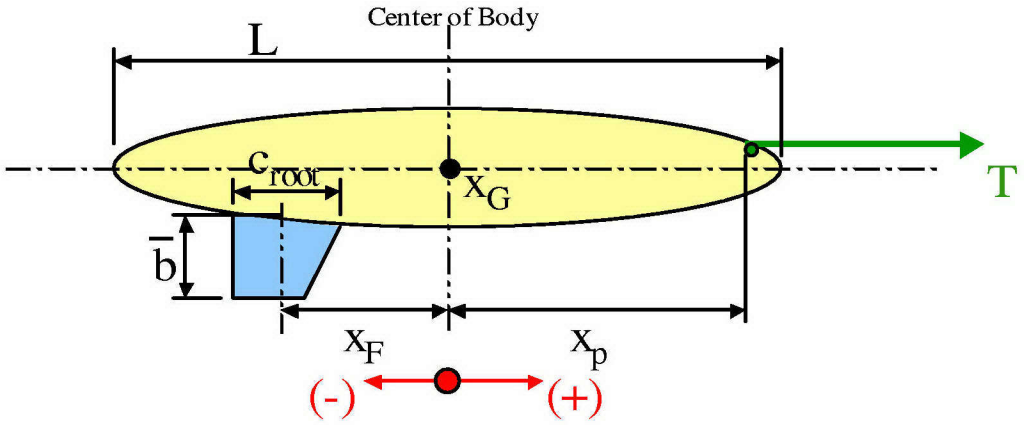

Figure 14. Towed Body

4. Root Chord Length (C'_{root})

The value for the root chord length determines the overall dimensions of the fin because the aspect ratio has already been assigned. The root chord length is also nondimensionalized with the length of the towed body. This variable will range from 0.02 to 0.3 at an interval of 0.01.

C. MATLAB PROGRAMMING

MATLAB version 7.0.1 was used to conduct the calculations for this thesis. In an effort to make the program easily tailored for a variety of variables, it was developed as a number of small programs for each individual component and type of calculation. This simplifies the effort required for the user to change the specifications for the body of revolution and the fins. It also allows additional components, such as the wings, to be easily added to the program. The hydrodynamic coefficients are calculated in an individual file, and the stability criterion are also calculated in an individual file. A separate file is used to run the entire program and assign the range of values for each of the variables through the use of several 'for' loops. The nested 'for' loops produce data for a total of 16,705 rudder configurations. All of this data is then stored in an array, and additional program files are used to develop the plots seen in Figures 15 through 37. The m.files developed to conduct these calculations may be reviewed in appendix A.

VI. RESULTS

A. R_1 STABILITY CRITERIA

The first condition evaluated is the R_1 stability criteria. This condition is independent of the tow cable tension, Towed Body resistance, and towing vessel's speed. The data shows that for each effective aspect ratio evaluated, there is a critical value for C'_{root} and x'_F for which the R_1 criteria is satisfied. Evaluated with no fins, the Towed Body does not meet the R_1 stability criteria. Table 3 summarizes the critical values for the R_1 stability criteria for the fin configurations examined in this study. The value identified as $x'_{F_{CRITICAL}}$ indicates the most forward position on the body which that fin may be located and still meet the R_1 stability criteria.

a	n=1		n=2	
	C'_{root}	$x'_{F_{CRITICAL}}$	C'_{root}	$x'_{F_{CRITICAL}}$
0.5	<0.13	All fail R_1	<.09	All fail R_1
	0.13	-0.44	0.09	-0.48
	0.14	-0.32	0.10	-0.30
	0.15	-0.22	0.11	-0.18
	0.16	-0.14	0.12	-0.06
	0.17	-0.04-	>0.12	All satisfy R_1
	>0.17	All satisfy R_1		
1.0	<0.07	All fail R_1	<0.05	All fail R_1
	0.07	-0.32	0.05	-0.30
	0.08	-0.14	0.06	-0.06
	>0.08	All satisfy R_1	>0.06	All satisfy R_1

1.5	<0.05	All fail R1	<0.03	All fail R_1
	0.05	-0.22	0.03	-0.48
	>0.05	All satisfy R_1	0.04	-0.06
			>0.04	All satisfy R_1
2.0	<0.04	All fail R_1	<0.03	All fail R_1
	0.04	-0.14	0.03	-0.06
	>0.04	All satisfy R_1	>0.03	All satisfy R_1
2.5	<0.03	All fail R_1	0.02	-0.30
	0.03	-0.22	>0.02	All satisfy R_1
	>0.03	All satisfy R_1		
3.0	<0.03	All fail R_1	0.02	-0.06
	0.03	-0.04	>0.02	All satisfy R_1
	>0.03	All satisfy R_1		
3.5	0.02	-0.32	All	Satisfy R_1
	>0.02	All satisfy R_1		
4.0	0.02	-0.12	All	Satisfy R_1
	>0.02	Satisfy R_1		
>4.0	All	Satisfy R_1	All	Satisfy R_1

Table 3. Critical Values for R_1 Stability Criteria

The data shows that as the effective aspect ratio increases, the size of the fin can decrease while meeting the stability requirement. Each step increase in effective aspect ratio yields a smaller fin which meets the requirement. With an aspect ratio greater than 4.0, all of the modeled fin configurations satisfy the R_1 stability criteria.

The data also demonstrates that increasing from one to two vertical control surfaces has an impact on the satisfaction of the R_1 criteria. For a given effective aspect ratio, the two fin configuration will meet the R_1 criteria with a smaller fin compared to the one fin configuration.

B. G'_h STABILITY COMPARISON

The R_1 condition is compared to the G'_h stability index for the same fin configurations. Although the G'_h equation is for use with a free running vessel, it has been computed for the Towed Body and compared with the R_1 results. Table 4 shows the G'_h and R_1 comparison for a=1 and C'_{root} =0.08. Due to the vast amount of data compiled, this small range of data is shown because it exhibits the typical response seen over the entire range of data where the transition from unstable to stable occurs for both R_1 and G'_h. As found by evaluating the R_1 criteria, a towed body with no vertical control surfaces does not meet the G'_h stability criteria.

Number of fins	effective aspect ratio	x'F	C'root	R1(1)	R1(2)	R1 satisfied? (0=no, 1=yes)	Gh
1	1	-0.04	0.08	0.48	0.54316	0	-2.7233
1	1	-0.06	0.08	0.48	0.52848	0	-2.4462
1	1	-0.08	0.08	0.48	0.51381	0	-2.1611
1	1	-0.1	0.08	0.48	0.49913	0	-1.8749
1	1	-0.12	0.08	0.48	0.48445	0	-1.5938
1	1	-0.14	0.08	0.48	0.46978	1	-1.3231
1	1	-0.16	0.08	0.48	0.4551	1	-1.0667
1	1	-0.18	0.08	0.48	0.44042	1	-0.82736
1	1	-0.2	0.08	0.48	0.42574	1	-0.60675
1	1	-0.22	0.08	0.48	0.41107	1	-0.40557
1	1	-0.24	0.08	0.48	0.39639	1	-0.22377
1	1	-0.26	0.08	0.48	0.38171	1	-0.06075
1	1	-0.28	0.08	0.48	0.36704	1	0.084473
1	1	-0.3	0.08	0.48	0.35236	1	0.21311
1	1	-0.32	0.08	0.48	0.33768	1	0.3265
1	1	-0.34	0.08	0.48	0.323	1	0.42603
1	1	-0.36	0.08	0.48	0.30833	1	0.51308
1	1	-0.38	0.08	0.48	0.29365	1	0.58893
1	1	-0.4	0.08	0.48	0.27897	1	0.65483
1	1	-0.42	0.08	0.48	0.2643	1	0.71189
1	1	-0.44	0.08	0.48	0.24962	1	0.76113
1	1	-0.46	0.08	0.48	0.23494	1	0.80348
1	1	-0.48	0.08	0.48	0.22026	1	0.83976
1	1	-0.5	0.08	0.48	0.20559	1	0.87072

Table 4. R_1 and G'_h Comparison for a=1, C'_{root} =0.08

In Table 4, a red zero for R_1 indicates that the Towed Body is unstable for that given fin configuration. In the G_h' column, a negative value is red and also indicates an unstable configuration. A cell is highlighted in yellow where the R_1 and G_h' stability conditions do not match.

The two stability criterion generally do not concur with which configuration is the critical value, marking the change from an unstable to stable Towed Body. However, both R_1 and G_h' exhibit similar behavior across the range of data, where the R_1 criteria is satisfied with a fin which is smaller or further forward on the Towed Body as compared to the G_h' value. This trend allows the G_h' values to be used as a means to validate the R_1 findings.

Figures 15 through 19 exhibit the effect of fin size and location on the value of G_h' for the range of effective aspect ratios evaluated in this study. Each figure displays a separate plot for one fin and two fins in order to demonstrate the effect that this variable has on the value of G_h'. Points on the curves which fall between zero and one in the figures represent a stable configuration.

These figures show that as the root chord length increases, the fin can be placed further forward on the body while meeting the G_h' stability requirement. Also, as the effective aspect ratio is increased, smaller sized fins satisfy the G_h' stability requirement. In addition, increasing from one to two fins allows smaller sized fins to meet the stability requirement, and for the same sized fins to meet the criteria further forward on the Towed Body.

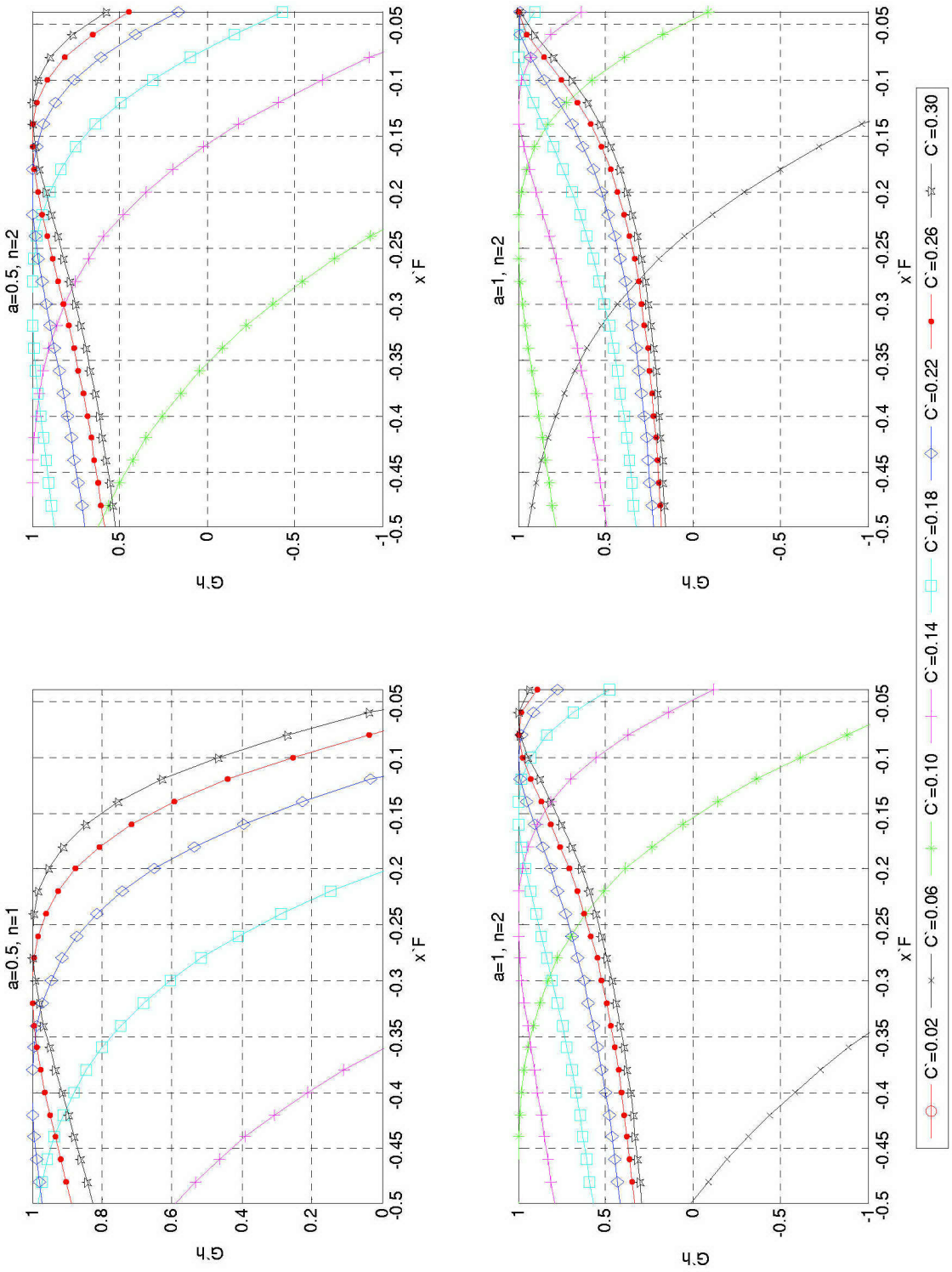

Figure 15. G'_h values for a=0.5 and 1.0

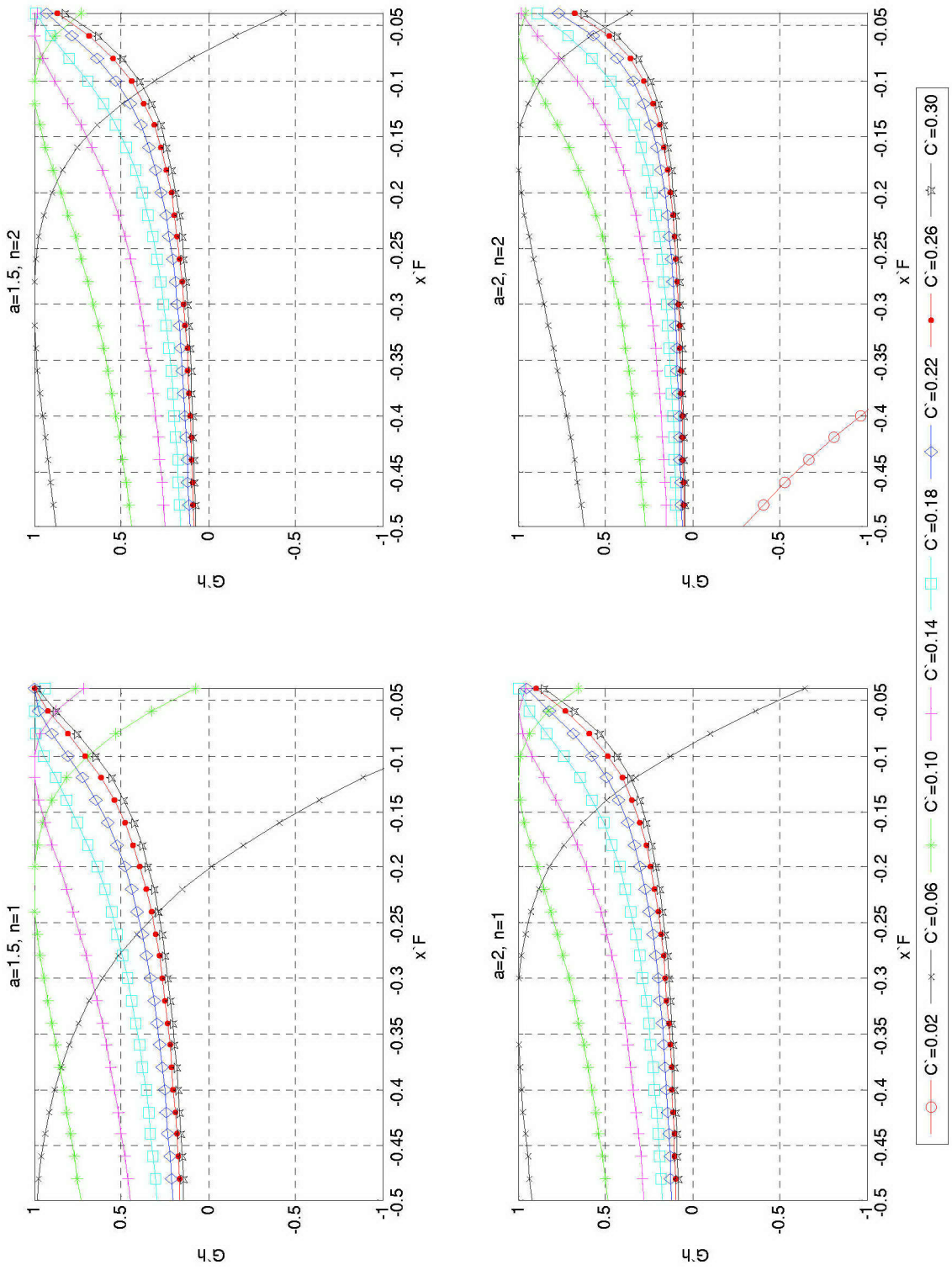

Figure 16. G'_h values for a=1.5 and 2.0

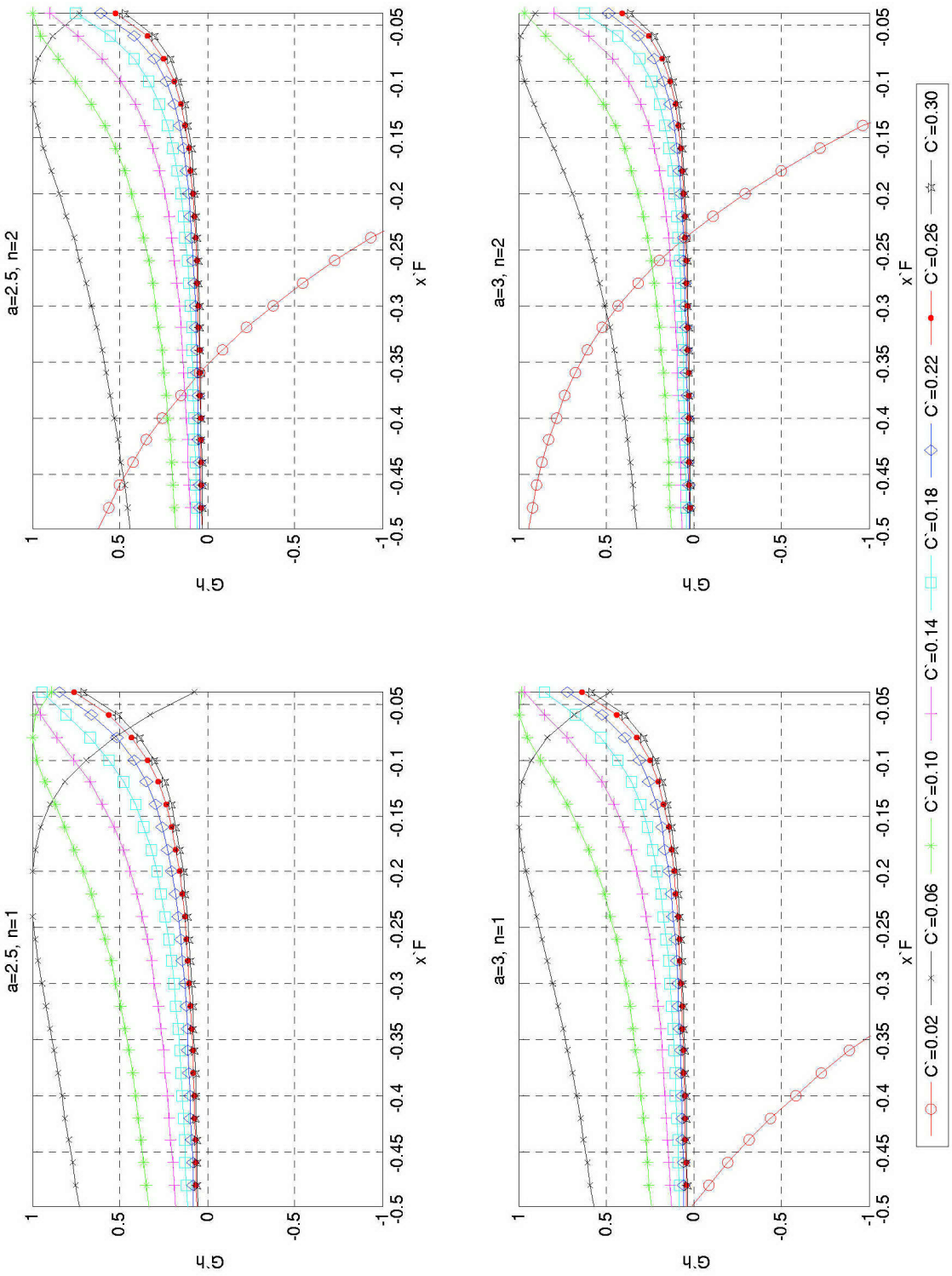

Figure 17. G'_h values for a=2.5 and 3.0

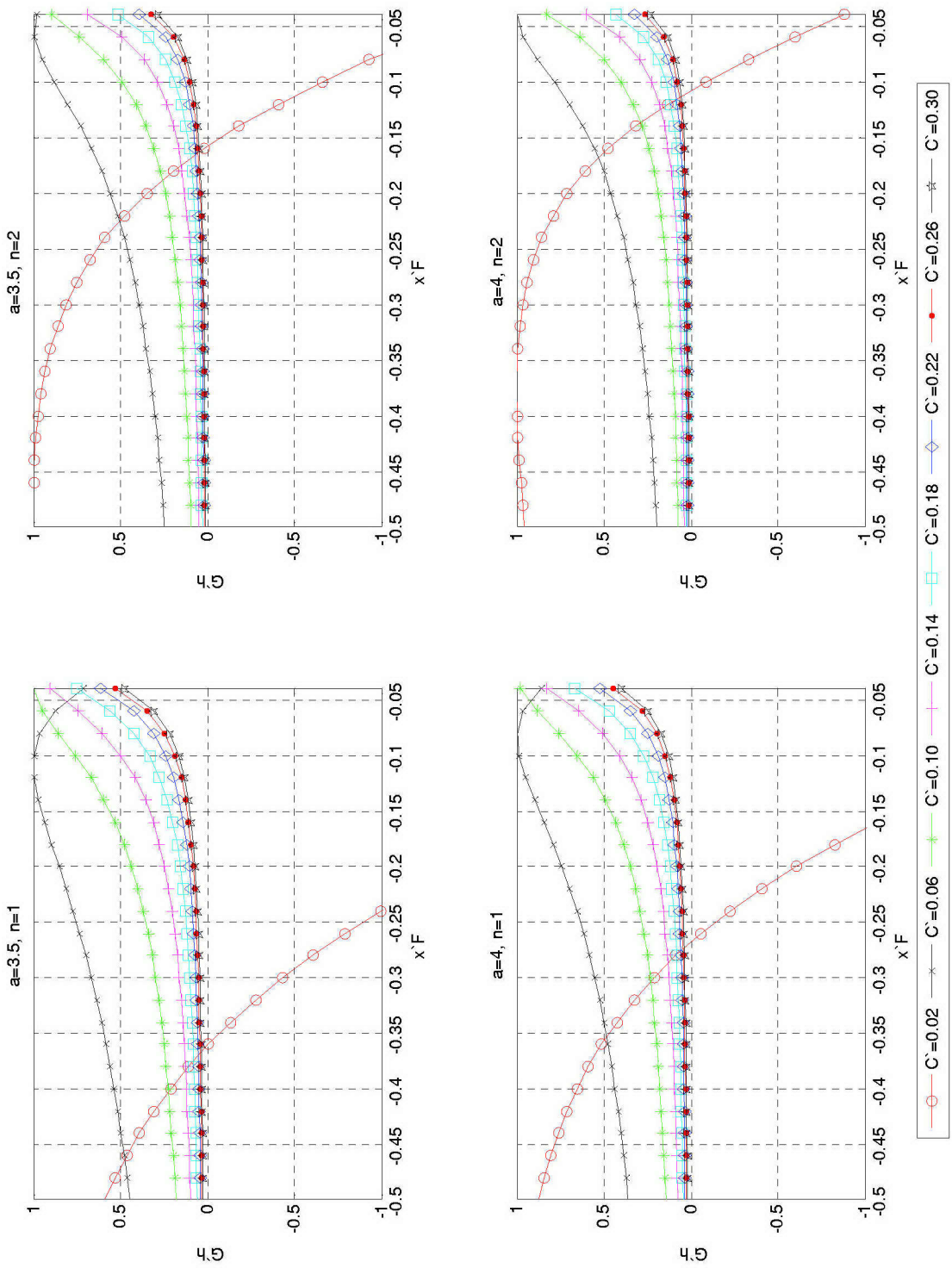

Figure 18. G'_h values for a=3.5 and 4.0

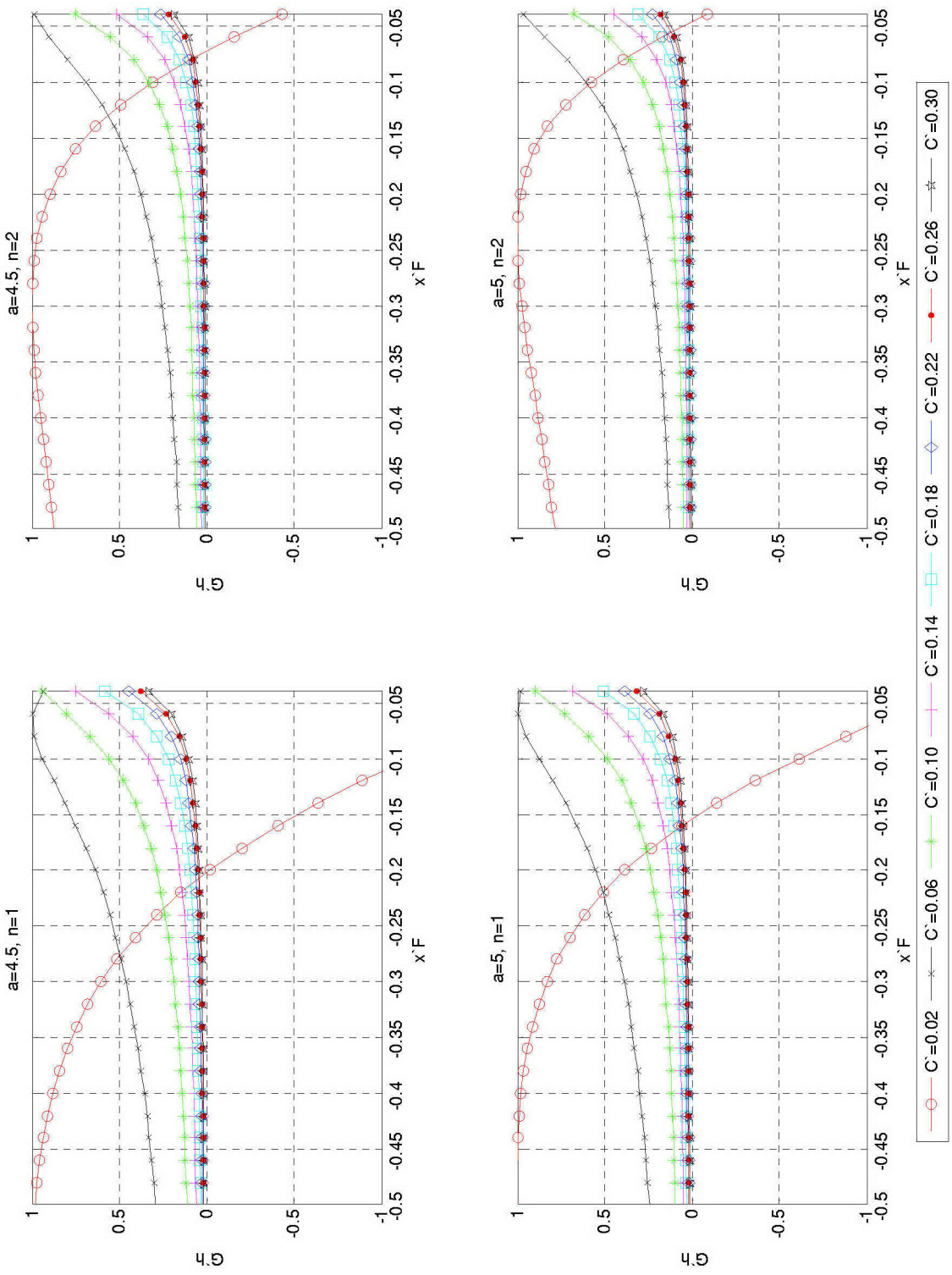

Figure 19. G'_h values for a=4.5 and 5.0

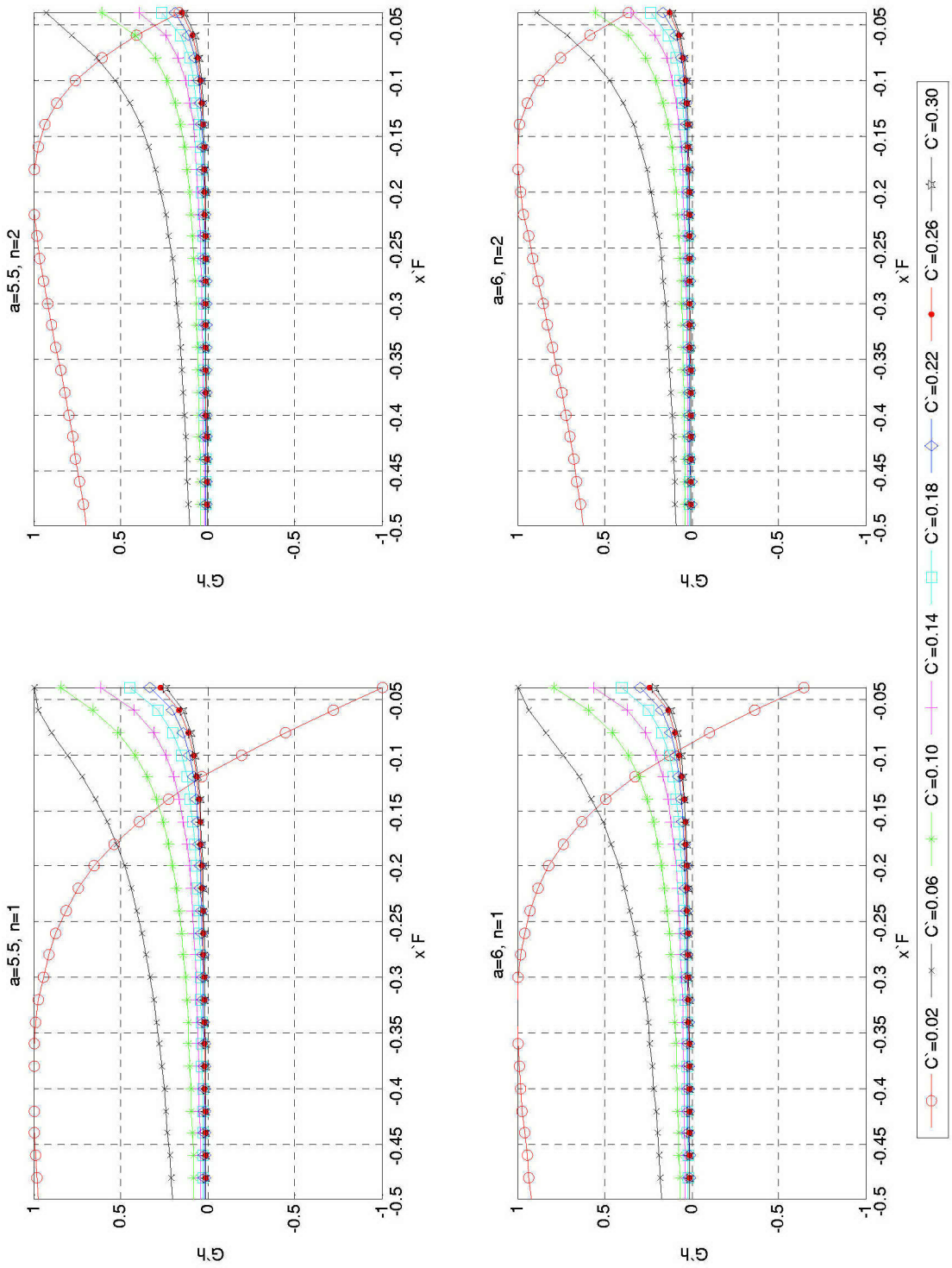

Figure 20. G'_h values for a=5.5 and 6.0

C. R_2 STABILITY CRITERIA

In order for the Towed Body to be evaluated as stable, both the R_1 and R_2 criterion must be satisfied. The R_2 stability criteria is dependent on the tow cable tension, which is a function of the Towed Body resistance and the speed of the towing vessel. Since this study is using a conceptual design for the Towed Body, actual tow cable tension values are difficult to accurately calculate. This is due to the lack of adequate design data to estimate the resistance of the Towed Body at various speeds. By using nondimensional values, the R_2 criteria can be evaluated to find the critical nondimensional tow cable tension (T'_{crit}) which is required to satisfy the stability criteria. The T'_{crit} values obtained in this study can be converted into a force if a Towed Body model is developed in detail. The force in the tow cable can then be used to determine minimum towing speeds required to meet the R_2 stability criteria.

This section presents numerous graphs showing how T'_{crit} is affected by varying the number of fins, the effective aspect ratio, the root chord length, and the longitudinal location of the fin. In any case where a value for T'_{crit} falls at or below zero, it can be assumed that particular Towed Body configuration will meet the R_2 criteria without any tension present in the tow cable. It is not possible for a negative tension to exist in the tow cable, as the physical cable will not permit a compression force of any significant magnitude to exist within the cable.

1. Impact of n on T'_{crit}

Figure 21 demonstrates the effect that the number of vertical control surfaces has on T'_{crit} for effective aspect ratios of one through four, with C'_{root} held constant. For a Towed Body without any fins, T'_{crit} is found to be less than zero. However, this configuration cannot be evaluated as being stable because with no fins, the Towed Body did not meet the R_1 criteria.

Comparing the curves for one and two fins, T'_{crit} is greater for the two fin configuration at any given longitudinal fin location. The graphs in Figure 21 also show that for both one and two fin configurations, the value for T'_{crit} decreases as the fin moves aft.

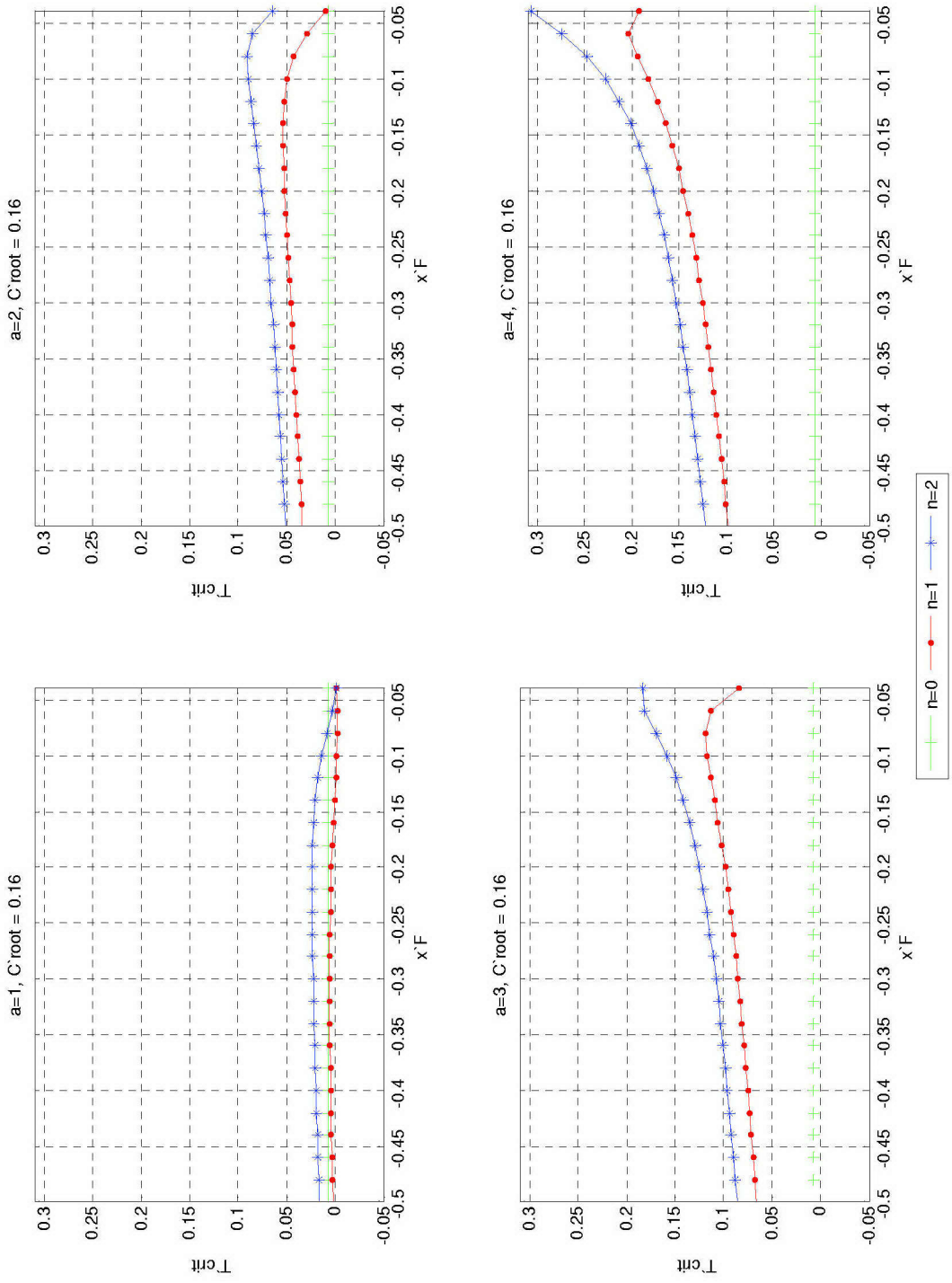

Figure 21. Effect of n on T'_{crit} for a = 1 to 4

2. Impact of a on T'_{crit}

a. T'_{crit} *vs.* x'_F

Figures 22 through 25 demonstrate the effect that the effective aspect ratio of a vertical control surface has on T'_{crit}. The figures show the effect for both one and two fin configurations.

Analysis of the graphs in Figures 22 and 23 shows that as the effective aspect ratio is increased, T'_{crit} will also increase. Also, as the fin is moved aft from an x'_F position of approximately -0.10, the value of T'_{crit} decreases for any given effective aspect ratio.

Comparing the graphs in figure 22 for one fin and figure 23 for two fins, it is also apparent that a higher value of T'_{crit} is calculated for two fins of a given size, aspect ratio, and location.

b. T'_{crit} *vs.* C'_{root}

Figures 24 and 25 also show the effect of increasing the effective aspect ratio, but in this case T'_{crit} is plotted against C'_{root} for specified values of x'_F. Here it is seen that for C'_{root} values generally less than 0.07, T'_{crit} falls below zero, indicating that the R_2 condition is satisfied with no tension in the tow cable.

As found in the previous section, an increase in the root chord length results in an increase in the corresponding values of T'_{crit}. However, the graphs in Figures 24 and 25 show this relation only holds true for C'_{root} values ranging from 0.05 to 0.12. As C'_{root} continues to increase beyond 0.12, there is minimal effect on T'_{crit} for any given effective aspect ratio.

As before, an increase in the number of fins produces a higher value of T'_{crit} with the same root chord length and location.

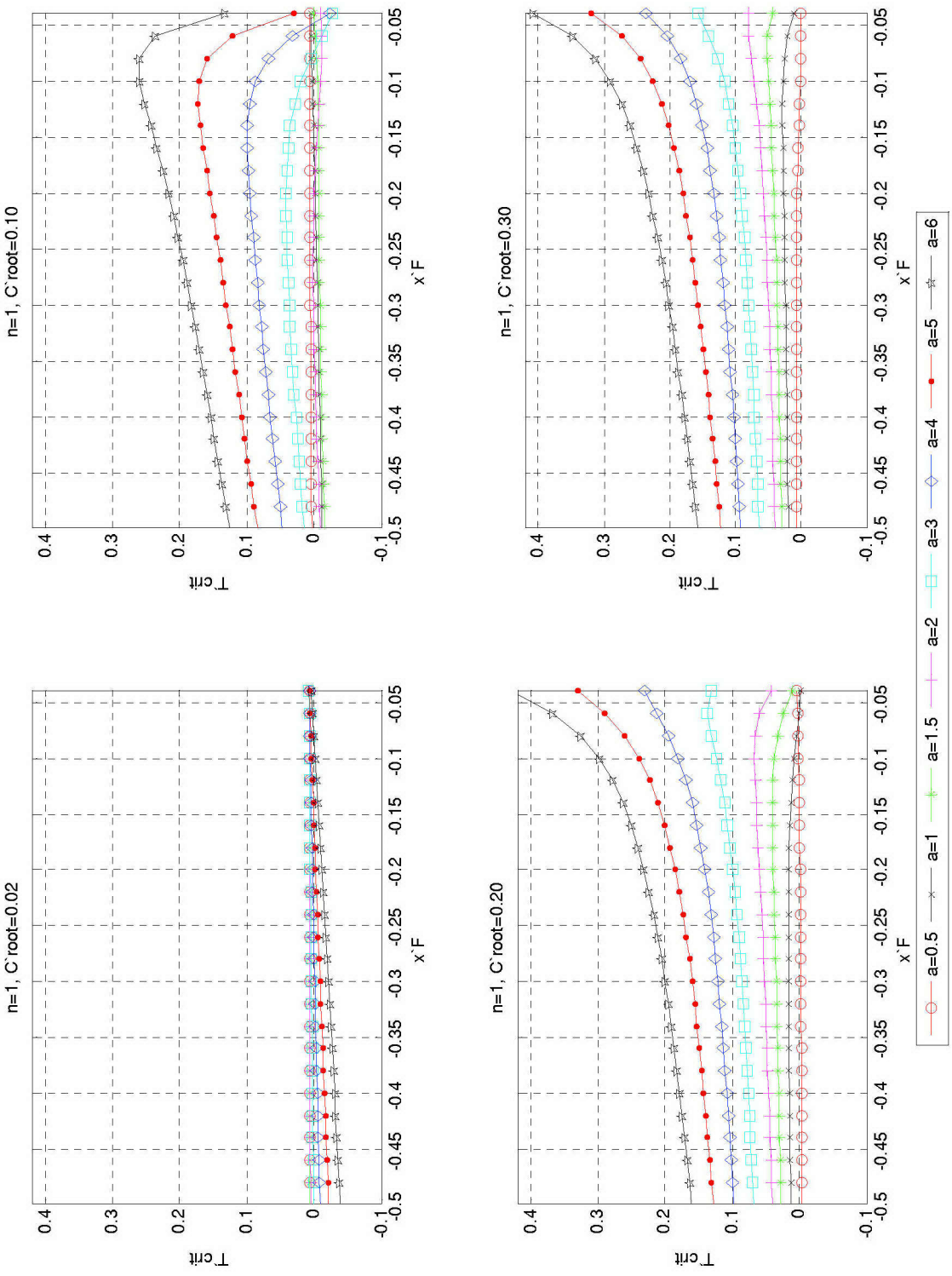

Figure 22. Effect of a on T'_{crit} for specified C'_{root} values, n = 1

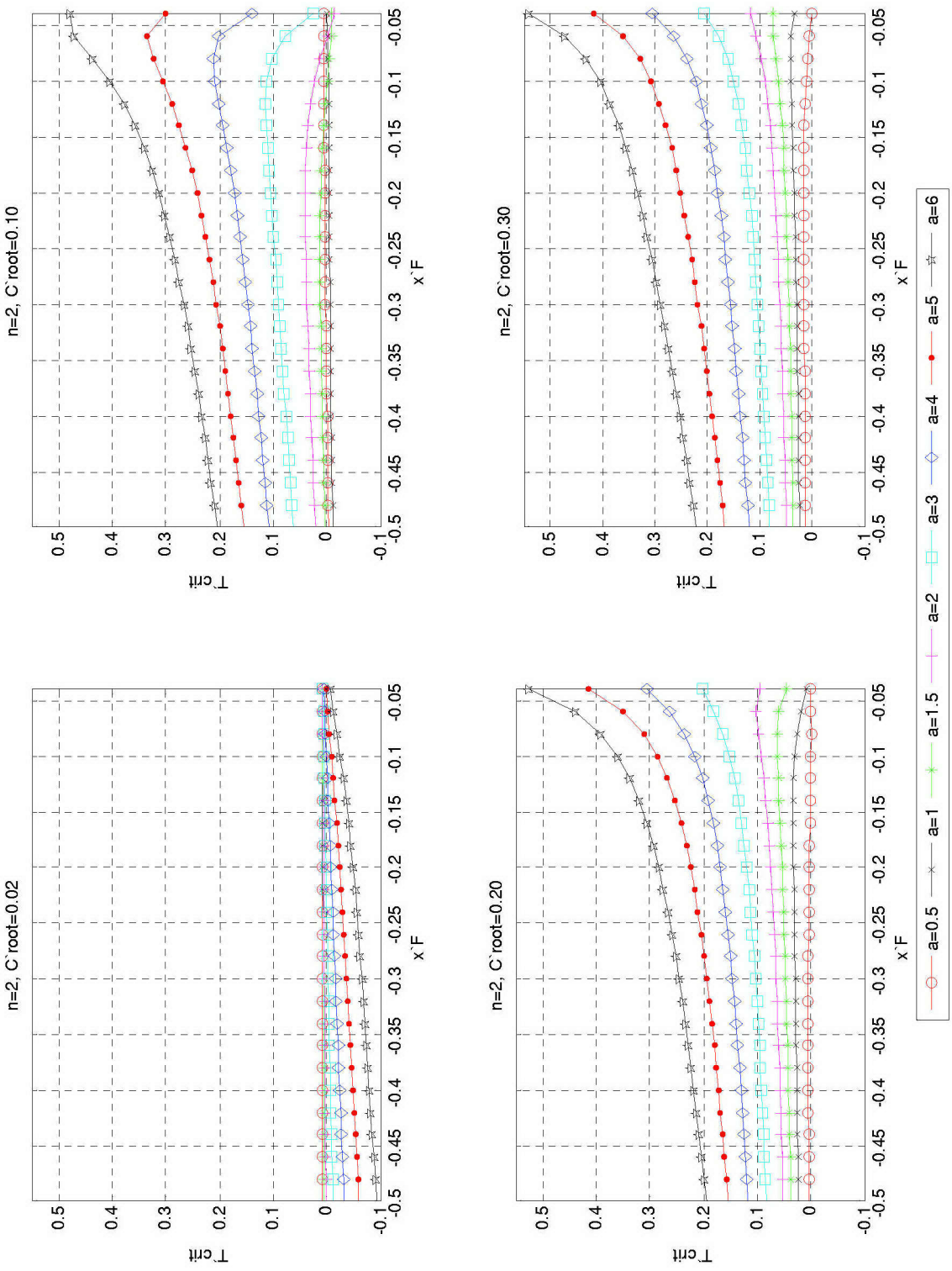

Figure 23. Effect of a on T'_{crit} for specified C'_{root} values, n = 2

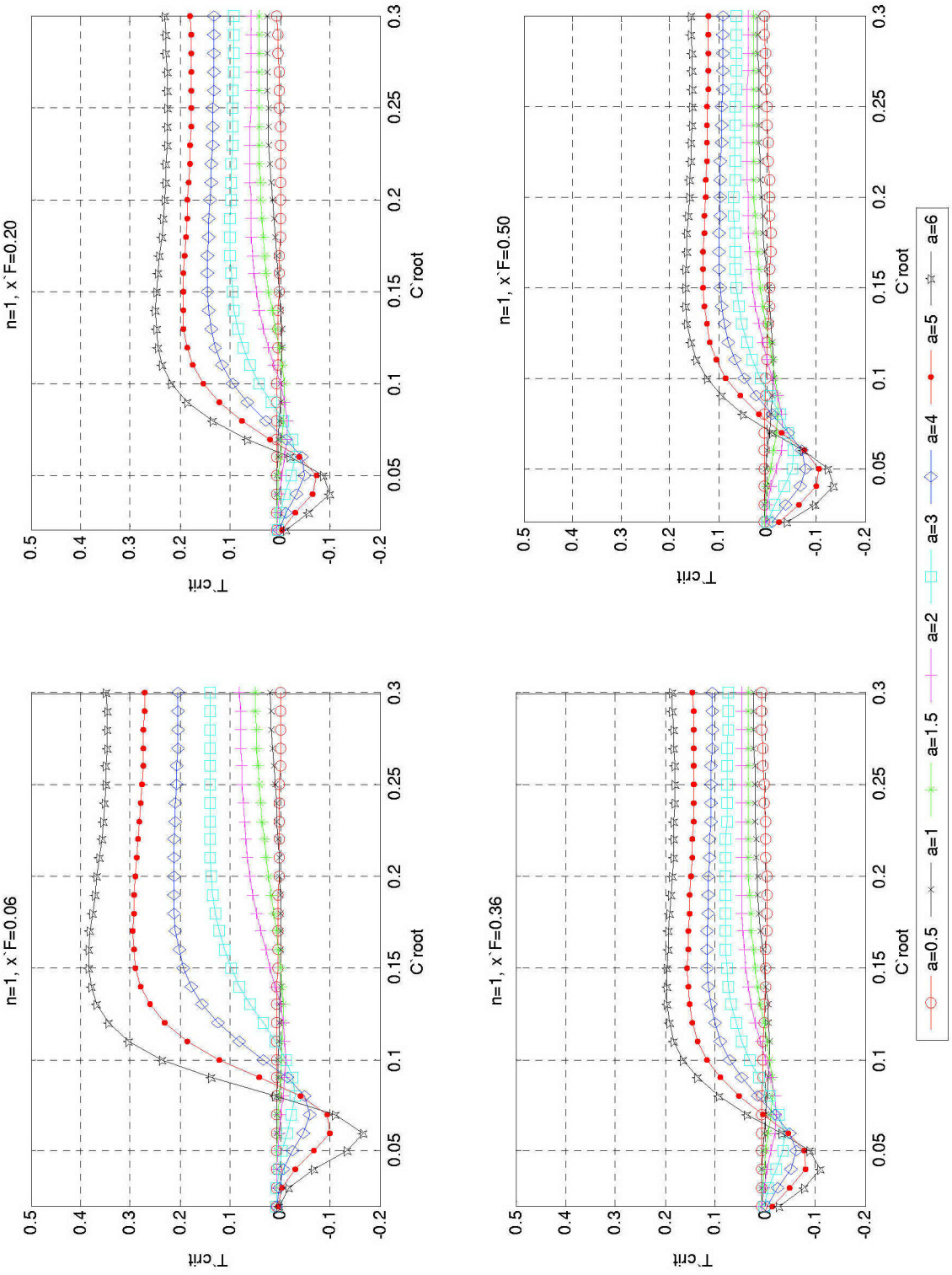

Figure 24. Effect of a on T'_{crit} for specified x'_F values, n = 1

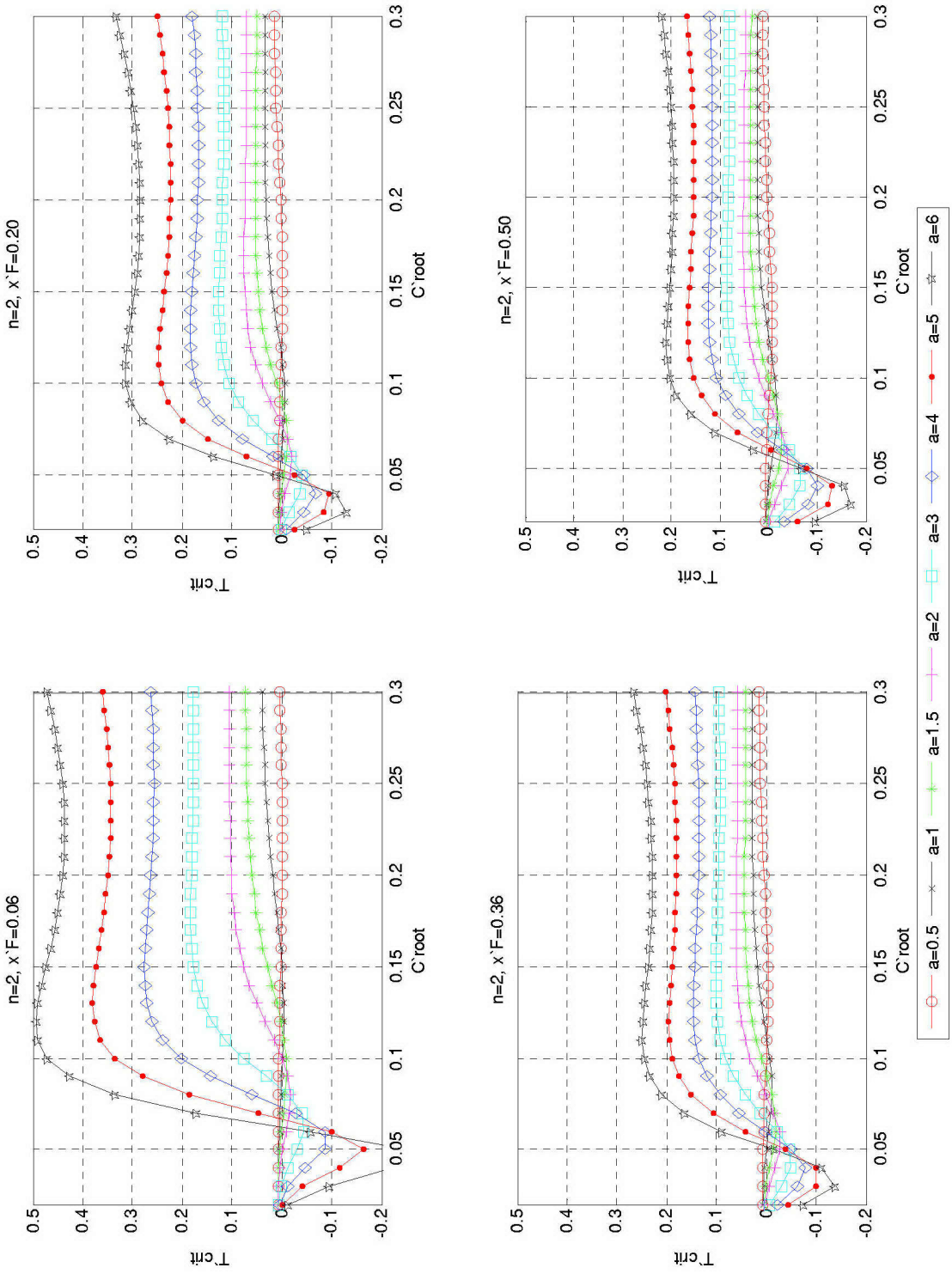

Figure 25. Effect of a on T'_{crit} for specified x'_F values, n = 2

3. Impact of C'_{root} on T'_{crit}

The impact which the size of the rudder has on the value of T'_{crit} is shown in Figures 26 through 31. In these figures, T'_{crit} vs. x'_F is plotted for specified values of C'_{root} and a for both one and two fin configurations.

It is apparent by examining these figures that T'_{crit} decreases as the fin is moved aft from an approximate x'_F position of -0.1. As x'_F approaches zero, or the center of the body, the T'_{crit} values experience a considerable shift for mid-range values of C'_{root}.

In general, T'_{crit} increases as the effective aspect ratio increases. Increasing from one to two fins also increases the corresponding T'_{crit} values. As expected, this concurs with the results from previously discussed figures.

Figures 26 through 31 exhibit an interesting trend for T'_{crit} based on C'_{root} and a. In Figure 27, the graph for a=1.5, n=1 shows that the upper limit for T'_{crit} corresponds with C'_{root} = 0.30. As C'_{root} decreases from 0.30 through the first three step intervals, the T'_{crit} values are near the T'_{crit} values for C'_{root} = 0.30. A significant shift in T'_{crit} values does not occur until C'_{root} decreases to 0.14.

Reviewing Figures 28 through 31 for n=1 and a increasing to 6.0, it is seen that the upper boundary of T'_{crit} values increases. Also, as a increases, the T'_{crit} values for decreasing values of C'_{root} approach the upper boundary of T'_{crit}. In Figure 28 for a=3 and n=1, a significant drop in T'_{crit} does not occur until C'_{root} = 0.10. The graph for a=6 and n=1 in Figure 31 shows that the T'_{crit} values for C'_{root} >0.06 all fall along the upper boundary for T'_{crit}.

The graphs for n=2 in Figures 28 through 31 show that the same trend occurs for a Towed Body with two fins. The difference from a Towed Body with one fin is that the upper boundary values for T'_{crit} are greater. Also, the T'_{crit} values for smaller sized fins approach the upper boundary of T'_{crit} values with lower effective aspect ratios compared to the corresponding configuration where n=1.

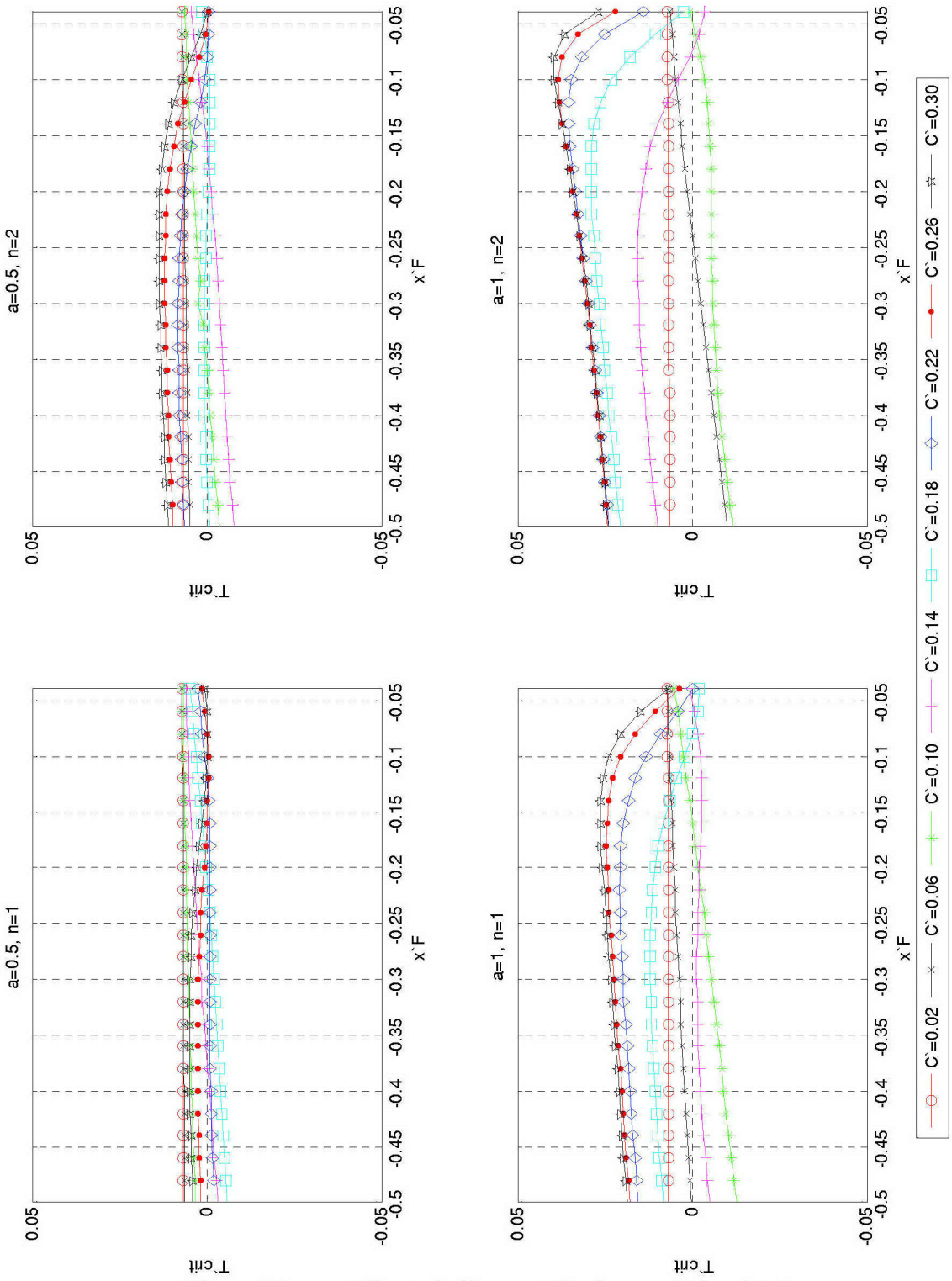

Figure 26. Effect of C'_{root} on T'_{crit} for a = 0.5 and 1.0

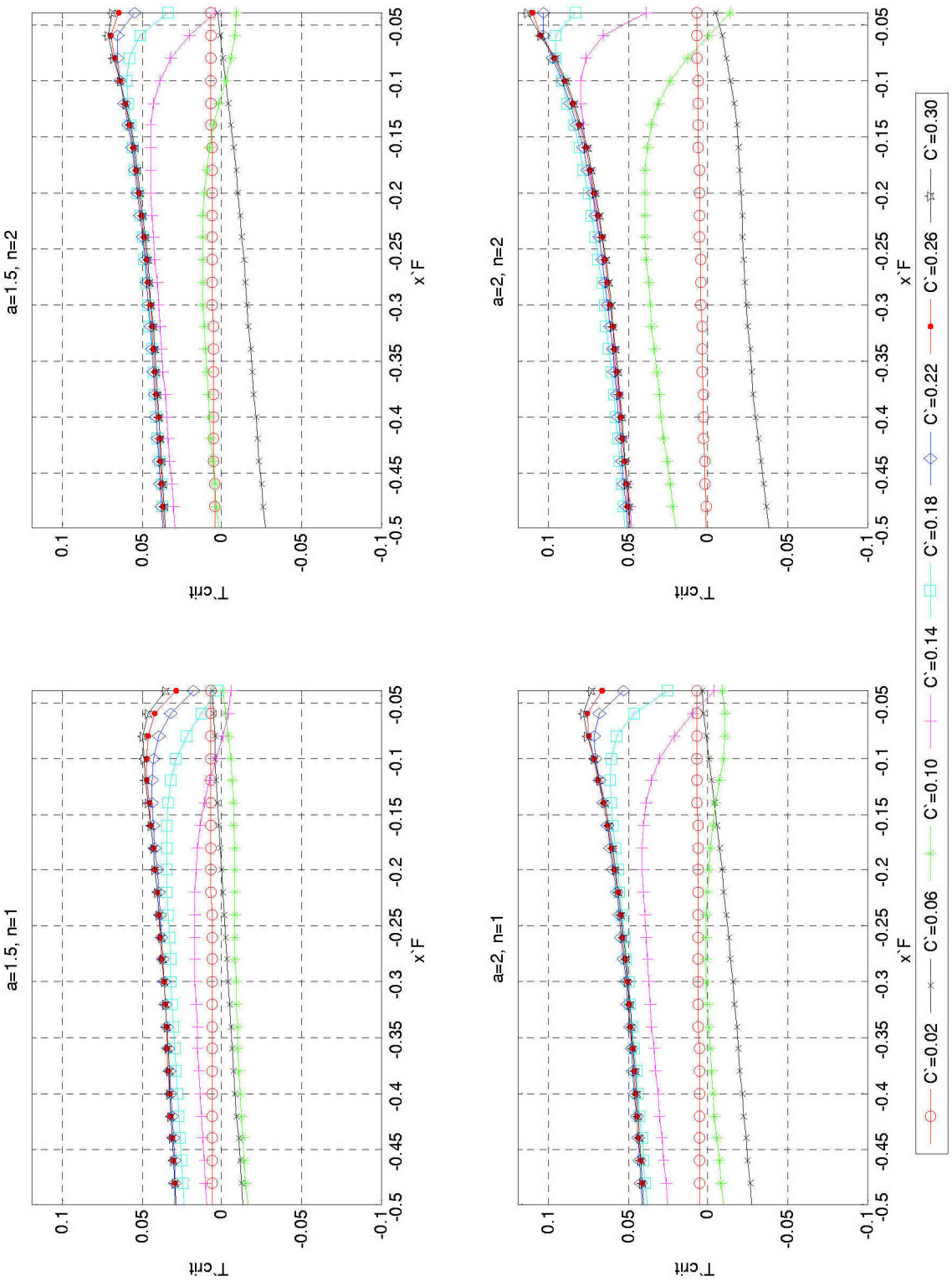

Figure 27. Effect of C'_{root} on T'_{crit} for a = 1.5 and 2.0

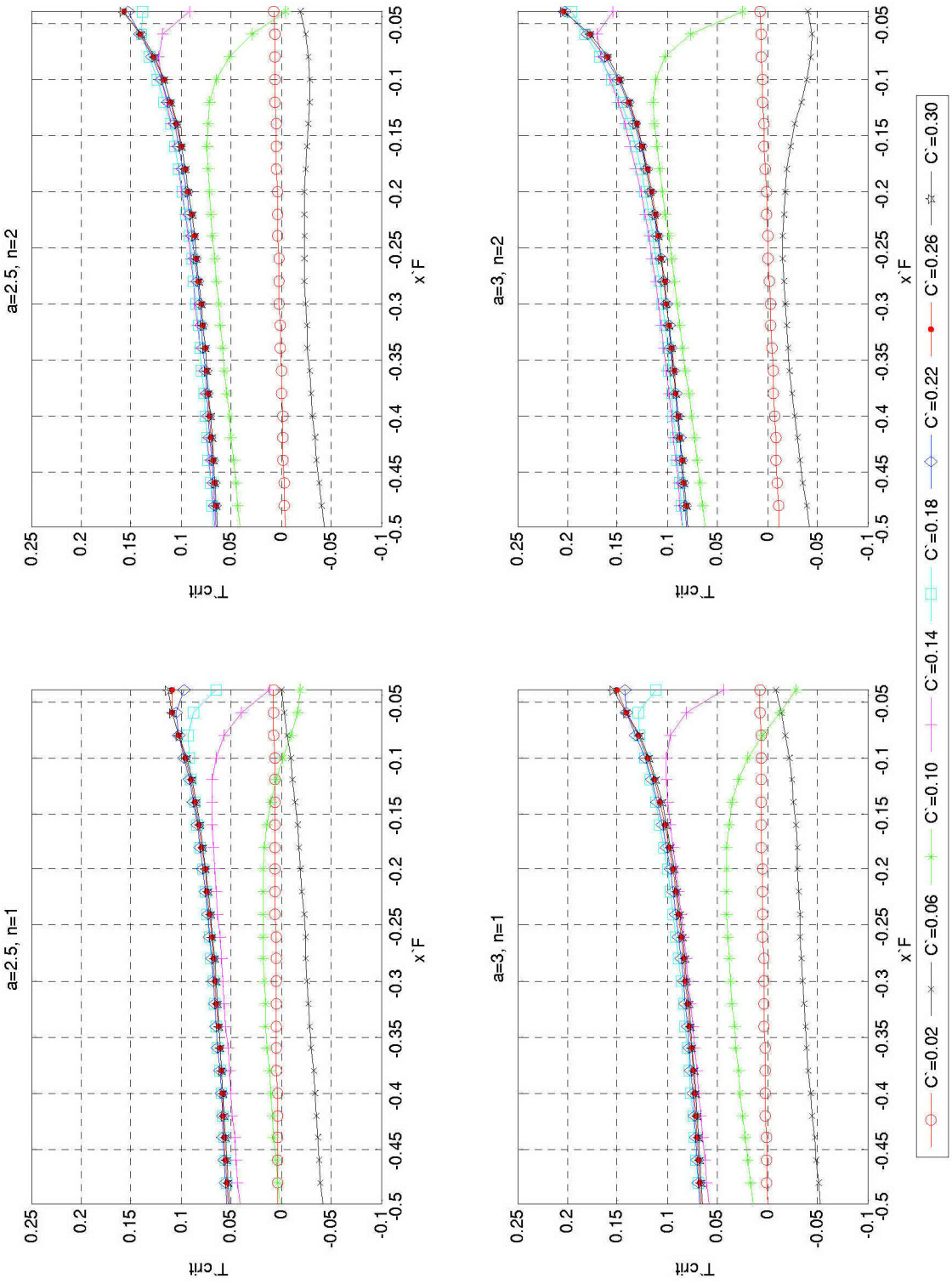

Figure 28. Effect of C'_{root} on T'_{crit} for a = 2.5 and 3.0

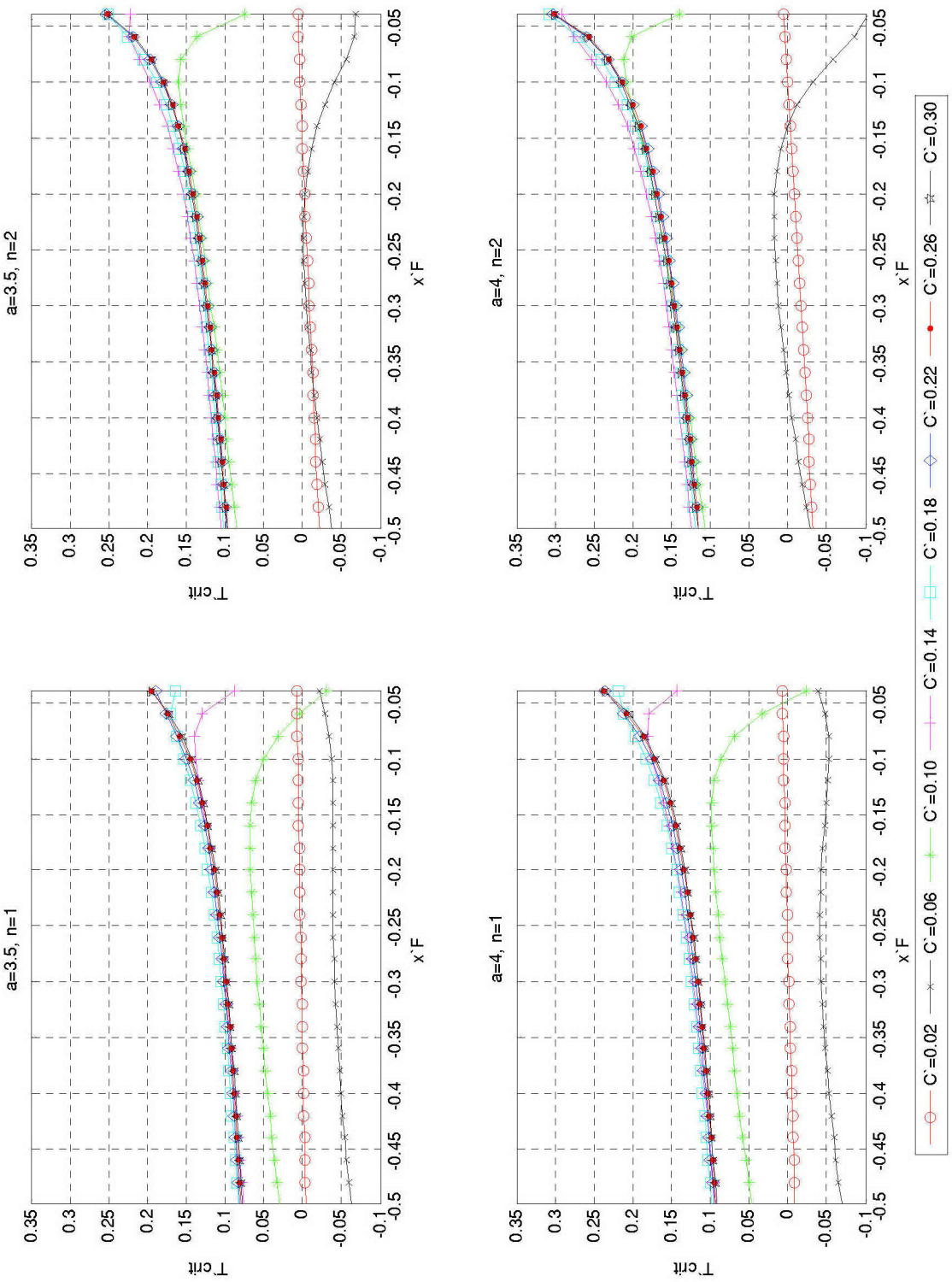

Figure 29. Effect of C'_{root} on T'_{crit} for a = 3.5 and 4.0

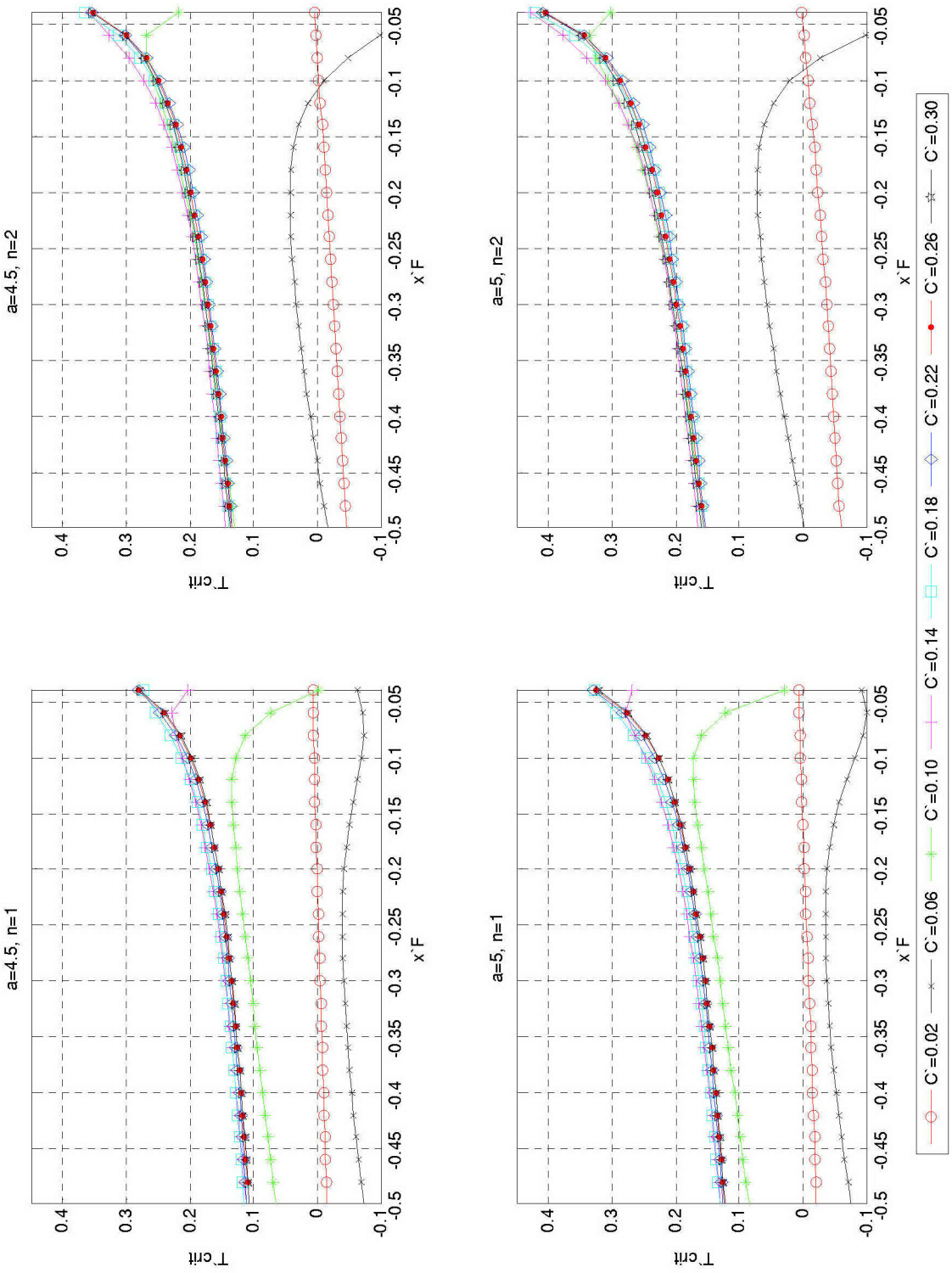

Figure 30. Effect of C'_{root} on T'_{crit} for a = 4.5 and 5.0

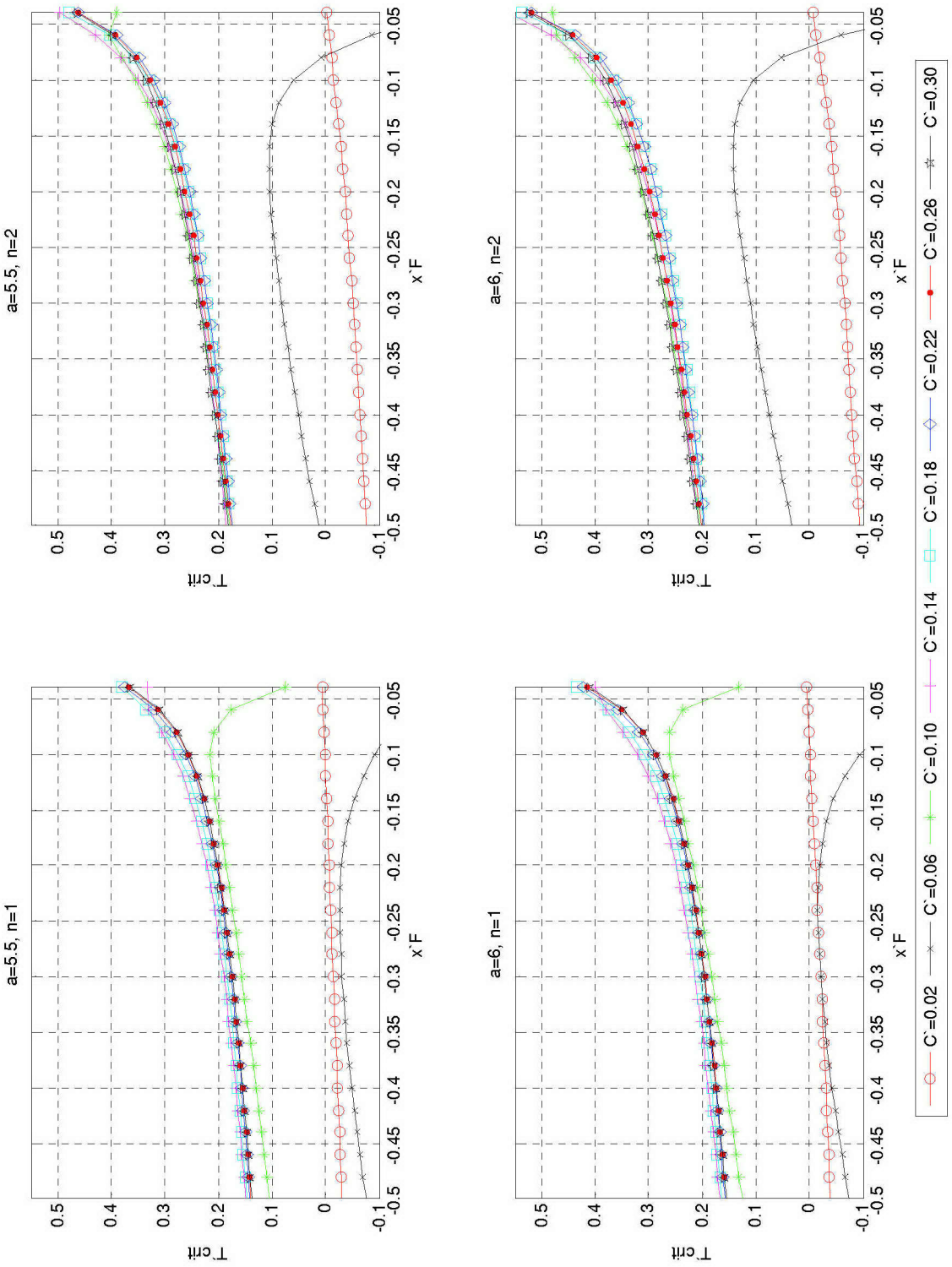

Figure 31. Effect of C'_{root} on T'_{crit} for a = 5.5 and 6.0

4. Impact of x'_F on T'_{crit}

The effect of moving the vertical control surface longitudinally on the Towed Body is presented in Figures 32 through 37. Here, T'_{crit} vs. C'_{root} is graphed for specified values of x'_F and a. The figures show this effect for one and two fin Towed Body configurations. The graphs in these figures show similar trends as seen in previous figures.

In most cases where C'_{root} is less than 0.10, T'_{crit} is less than or equal to zero, indicating that no tow cable tension is necessary to satisfy the R_2 criteria. Before assuming stability, the fin configuration must be checked against the R_1 criteria from Table 3. Where C'_{root} is less than 0.10 for lower effective aspect ratios, the R_1 criteria is often not satisfied.

As demonstrated in previous figures, T'_{crit} increases as the effective aspect ratio increases for C'_{root} values greater than 0.10. Also, T'_{crit} values for n=2 are higher than corresponding fin configurations for n=1.

As C'_{root} increases above 0.15 up to 0.30, the T'_{crit} values become somewhat constant. In this range for C'_{root}, the graphs show that T'_{crit} decreases as x'_F increases. This trend corresponds with the results seen in Figures 26 through 31.

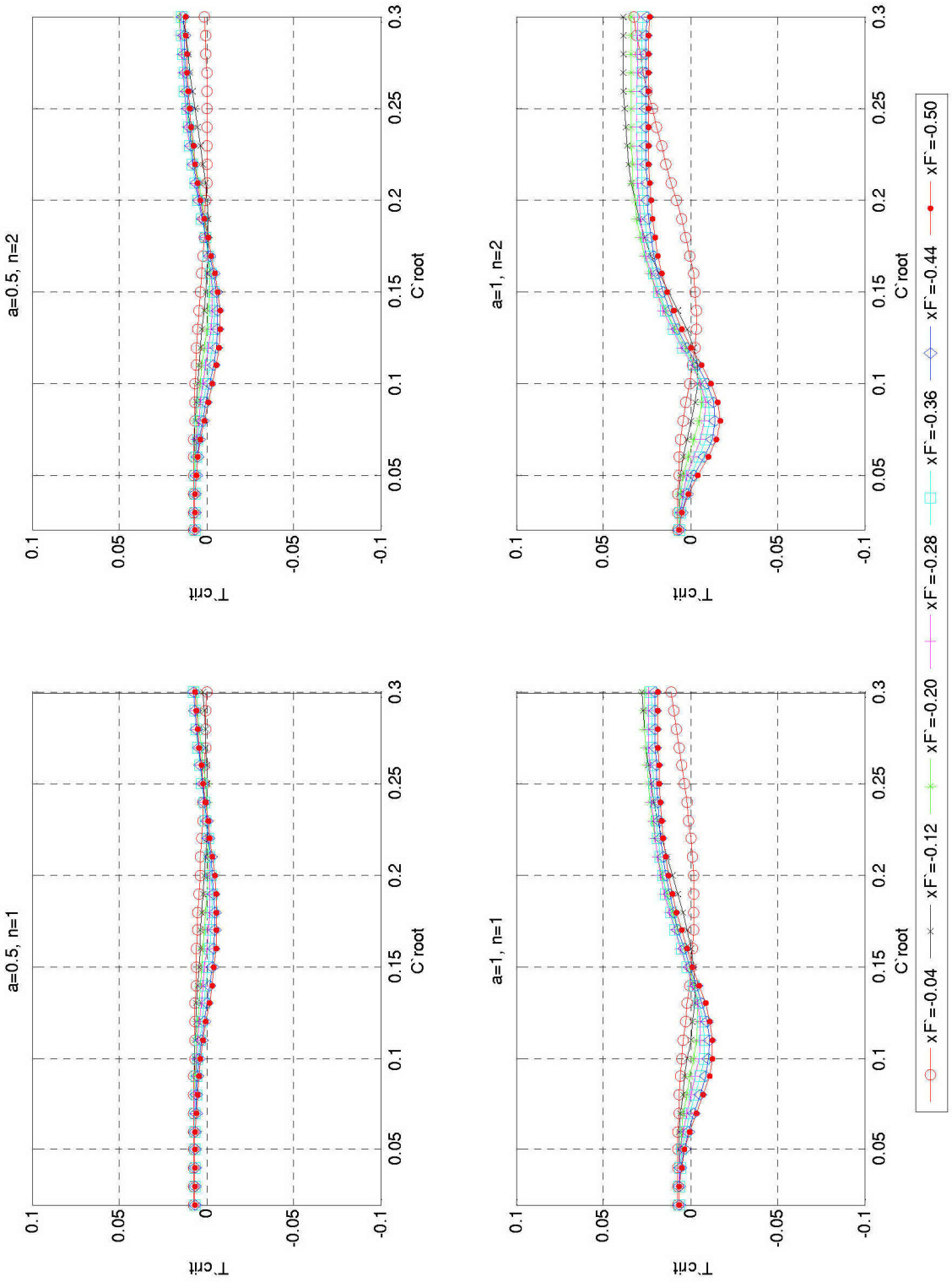

Figure 32. Effect of x'_F on T'_{crit} for a = 0.5 and 1.0

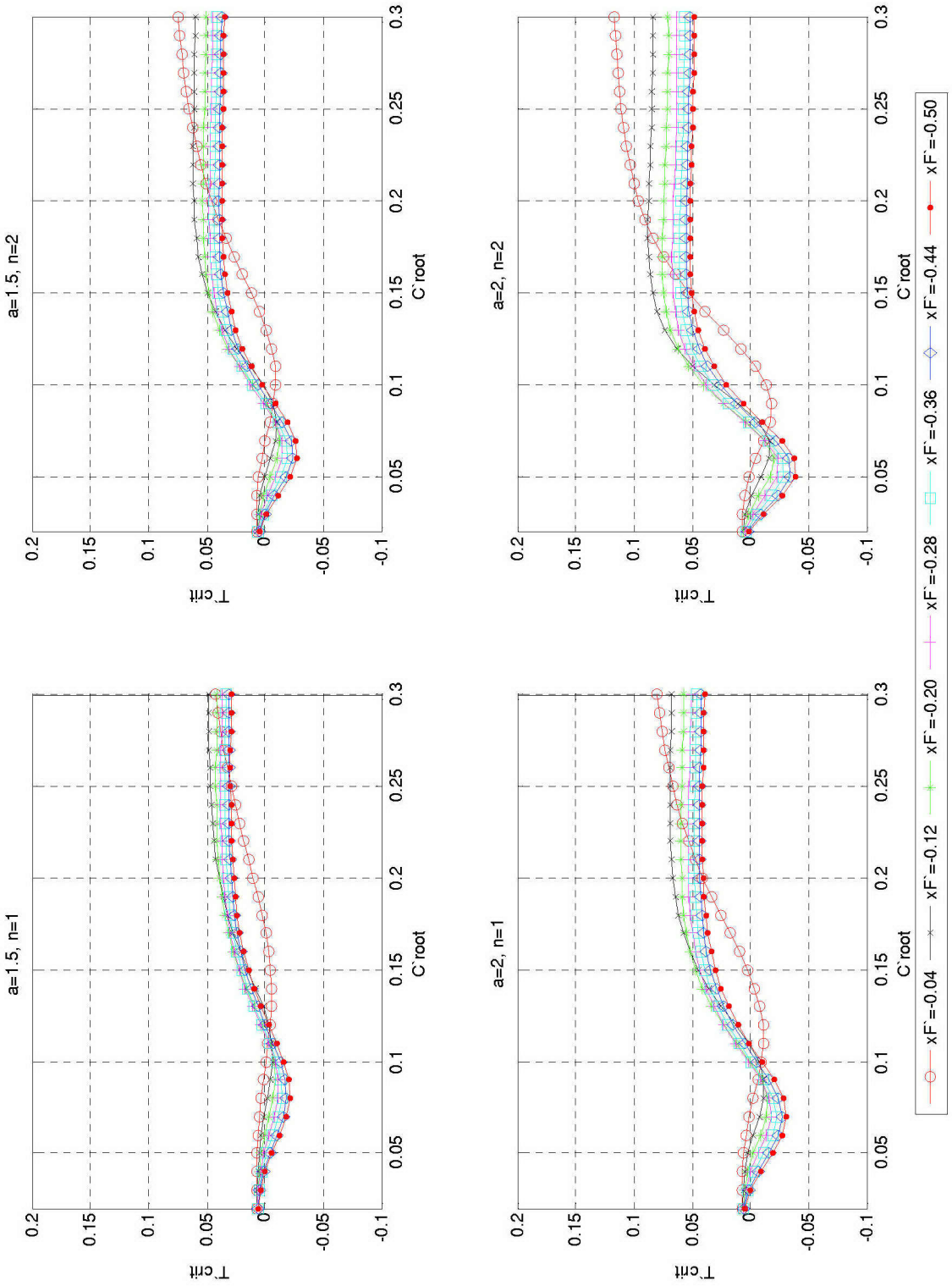

Figure 33. Effect of x'_F on T'_{crit} for a = 1.5 and 2.0

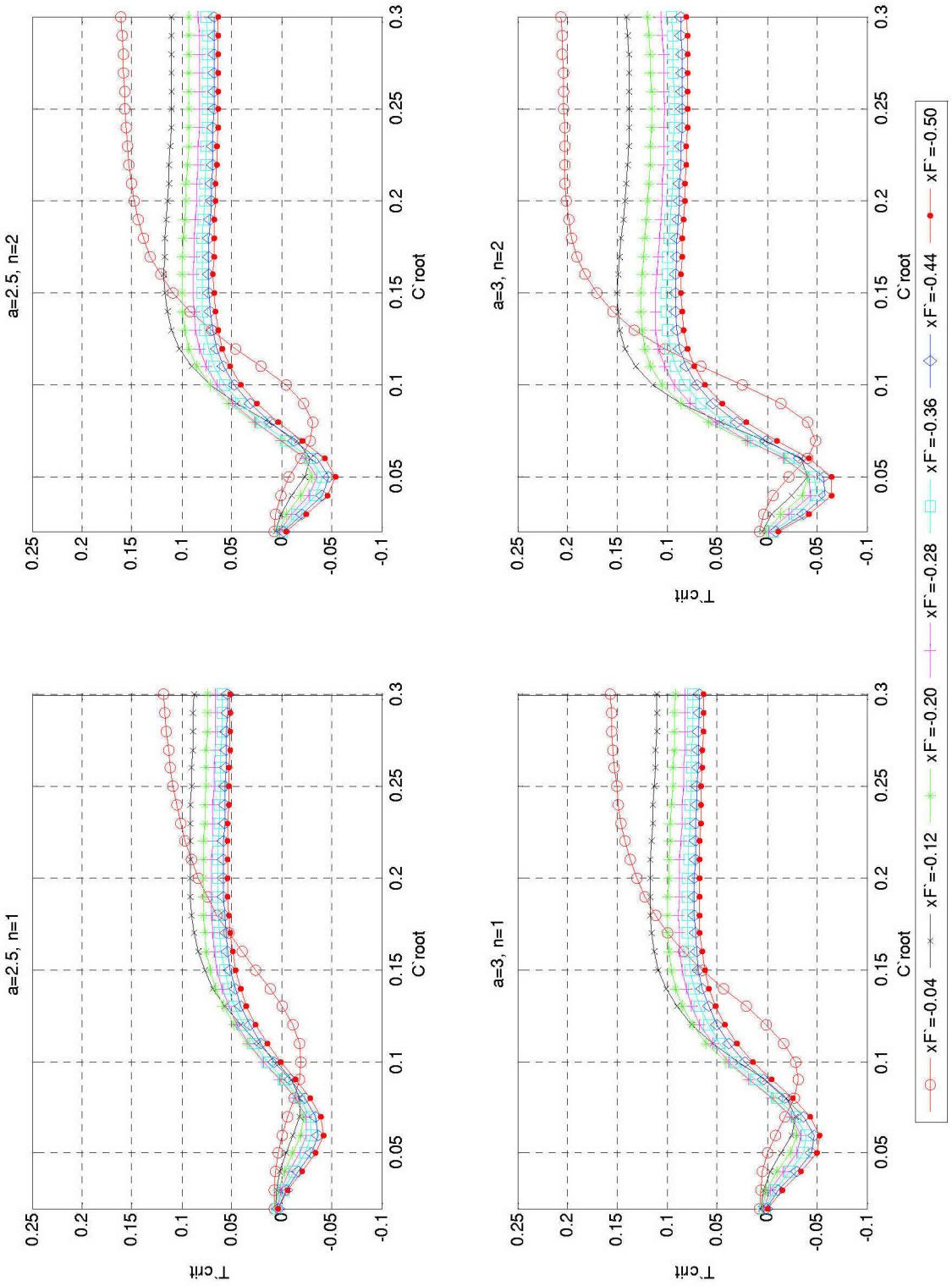

Figure 34. Effect of x'_F on T'_{crit} for a = 2.5 and 3.0

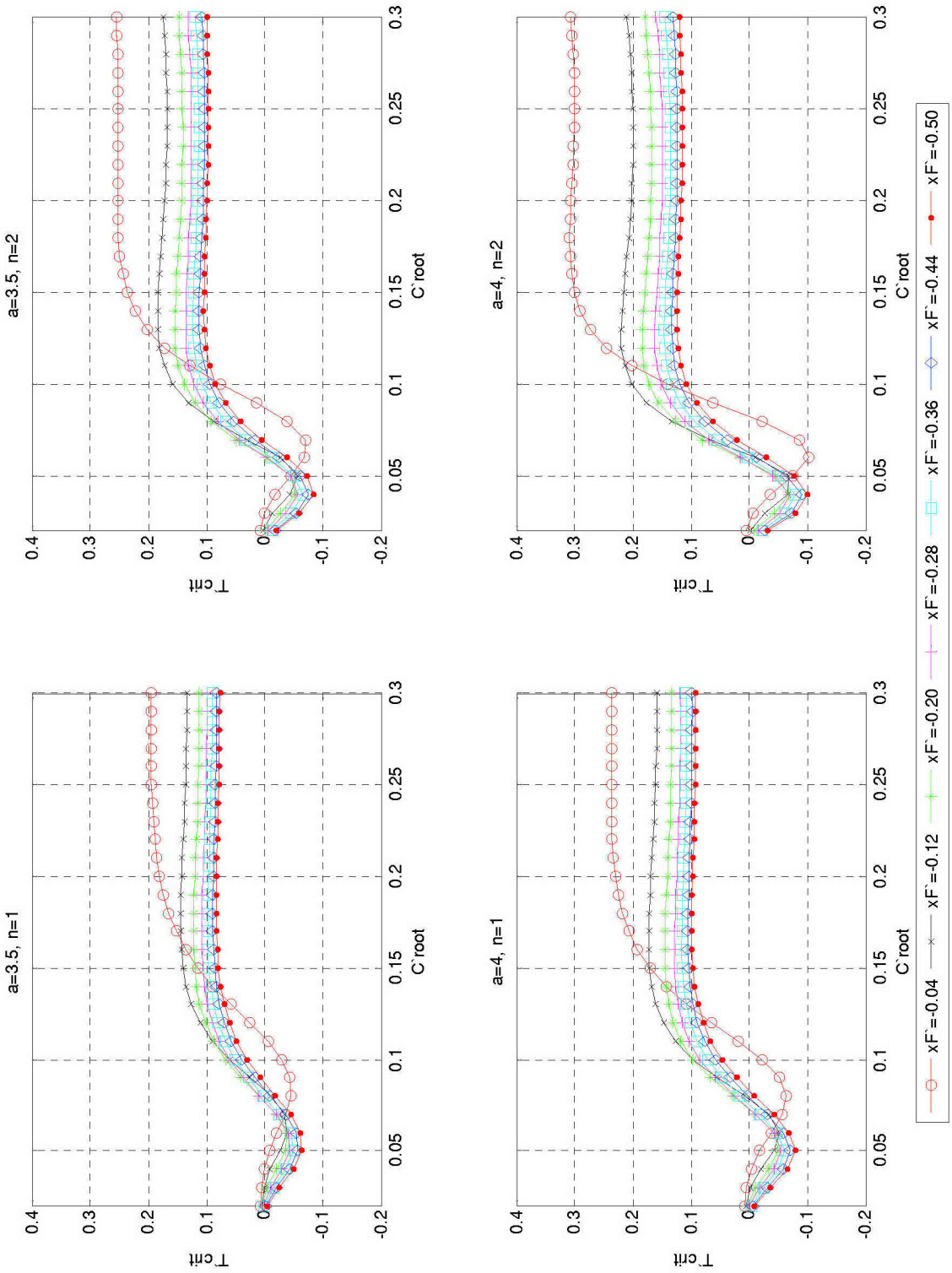

Figure 35. Effect of x'_F on T'_{crit} for a = 3.5 and 4.0

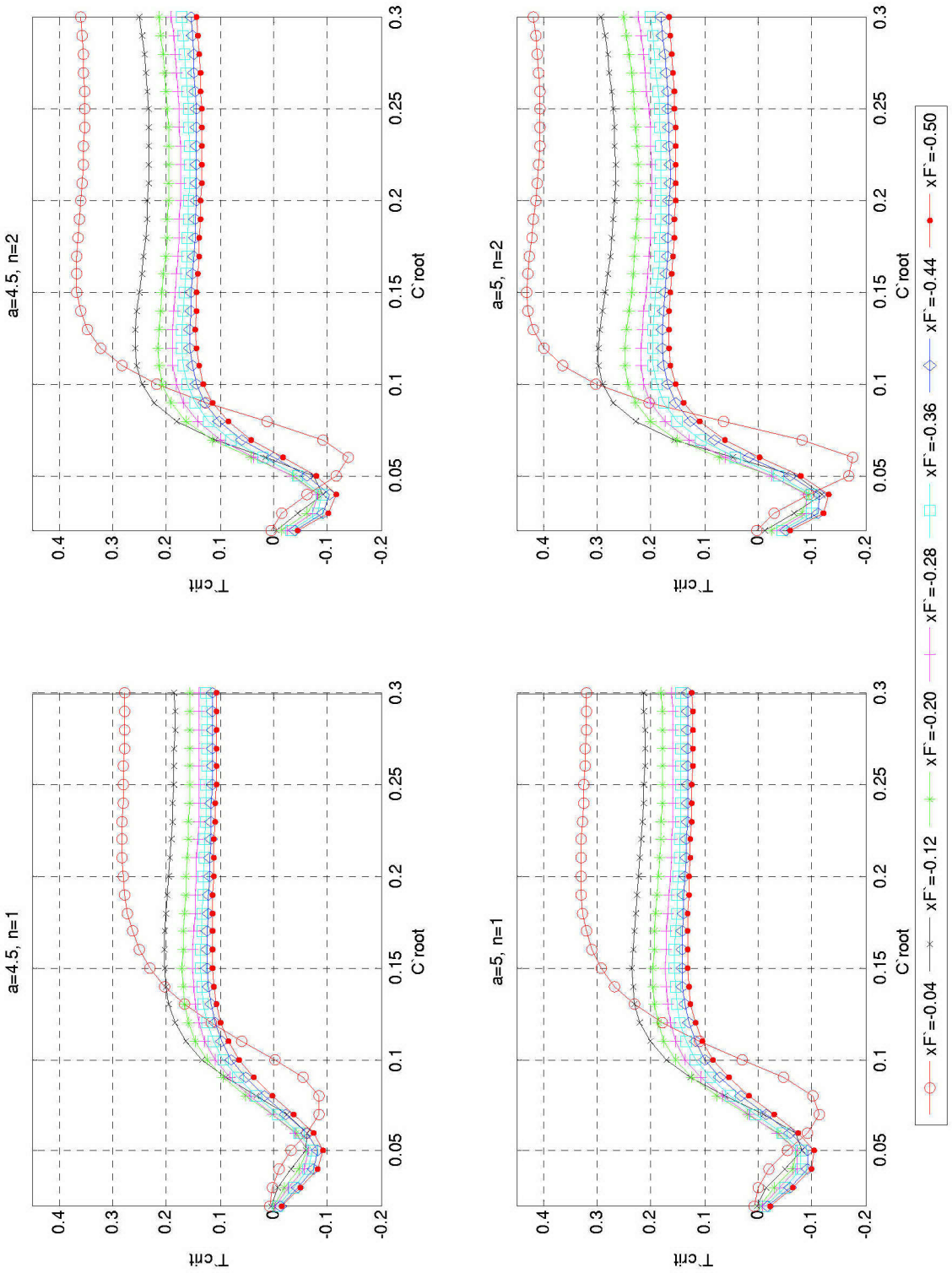

Figure 36. Effect of x'_F on T'_{crit} for a = 4.5 and 5.0

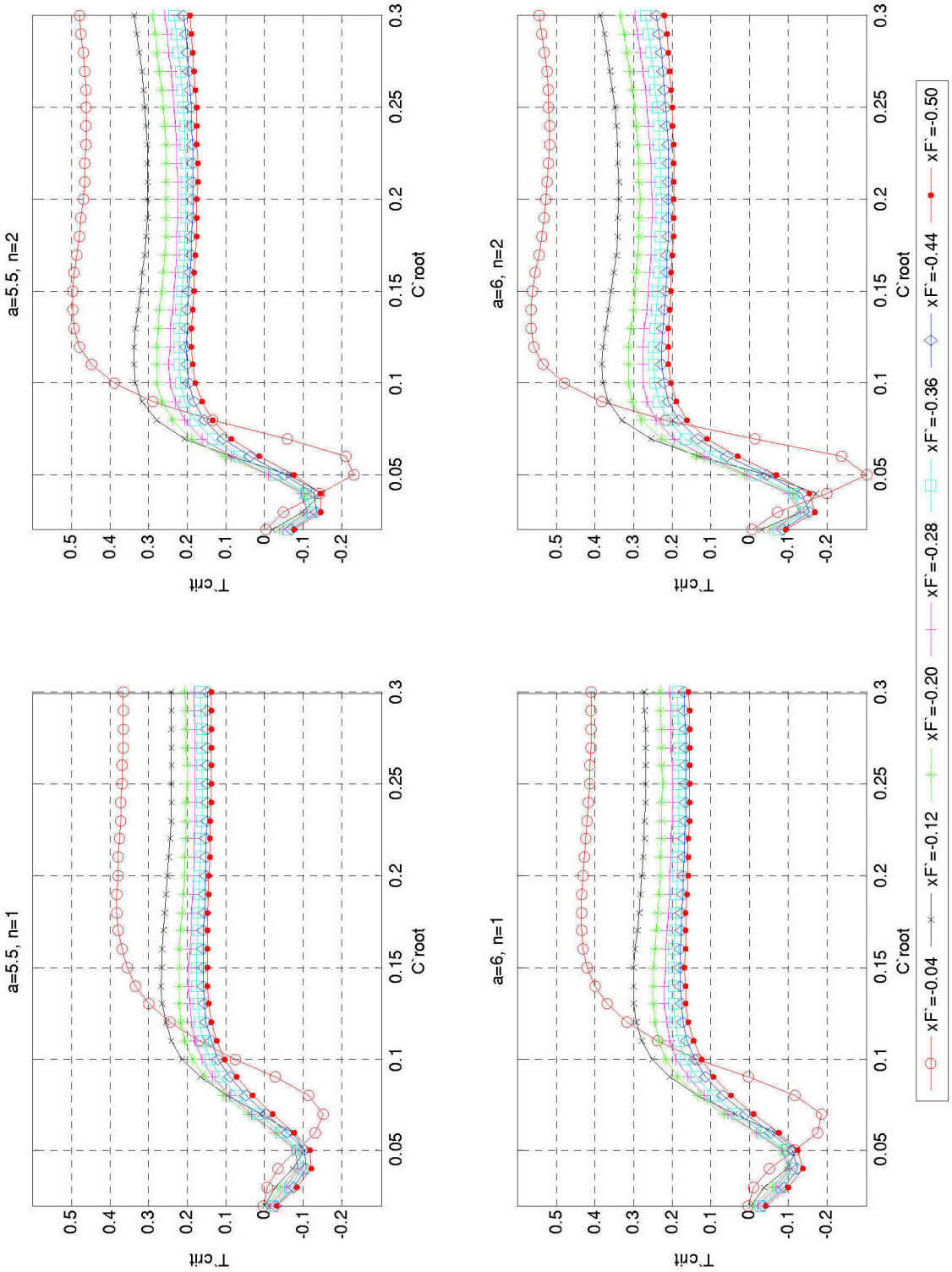

Figure 37. Effect of x'_F on T'_{crit} for a = 5.5 and 6.0

THIS PAGE INTENTIONALLY LEFT BLANK

VII. CONCLUSIONS AND RECOMMENDATIONS

A. CONCLUSIONS

This study evaluated the motion stability of the Towed Body LARS with a variety of fin configurations. To evaluate towing stability, the R_1 and R_2 stability criterion were assessed for each fin configuration. The R_1 criteria was also compared with the G'_h stability index for a free running vessel.

Examination of the critical values for R_1 in Table 3 and the graphs in Figures 15 through 20 finds predictable trends in meeting this stability criteria.

- The further aft a fin is placed on the Towed Body, the more likely it is to be stable.
- Increasing fin size allows the fin to be placed further forward and/or have a lower effective aspect ratio while meeting the stability criteria.
- Increasing the effective aspect ratio allows the fin to be placed further forward and/or be smaller in size while meeting the stability criteria.
- Adding additional fins reduces the minimum effective aspect ratio and fin size necessary to meet the stability criteria. It also allows the fins to be placed further forward.

Evaluation of the R_2 stability criteria yields critical values for the nondimensional tow cable tension. The data displayed in Figures 21 through 37 also show predictable trends for the minimum value of T' required to meet this stability criteria. The following conclusions are for fin configurations placed between the stern and a distance of 10% of the Towed Body's length aft of the center of the body ($-0.50 \le x'_F \le -0.10$).

- The use of multiple fins of the same size and effective aspect ratio yields a higher T'_{crit}.
- An increase in effective aspect ratio will increase T'_{crit}.

- Increasing the root chord length of a fin while holding the effect aspect ratio constant has little effect on T'_{crit} for a root chord length greater than approximately 15% of the Towed Body's length (C'_{root} >0.15).

- T'_{crit} decreases as a fin is moved aft from a position of x'_F =-0.10 towards the stern.

In order for the Towed Body to possess motion stability, both the R_1 and R_2 criterion must be satisfied. While a smaller size and lower effective aspect ratio fin design permits a lower nondimensional tow cable tension to pass the R_2 criteria, it is less likely to satisfy the R_1 criteria. However, as the fin is placed further aft on the Towed Body, the R_1 criteria is more likely to be satisfied and a lower nondimensional tow cable tension is necessary to satisfy the R_2 criteria.

B. RECOMMENDATIONS

There is a great deal of additional study to be conducted on the design of the Towed Body. The work conducted in this paper only addressed motion in the x-y plane, and focused on just two degrees of freedom: sway and yaw. Since the Towed Body concept is for both USV and UUV operations, the wings should be modeled and motion stability analysis should be conducted for pitch and heave. The effect of environmental forces on the motion stability may also be addressed in future work.

Once a detailed model of the Towed Body is developed where weights and dimensions are known, the R_2 criteria may be used to determine specific operating requirements, such as towing speed and the necessary capacity of the tow cable. Subsequent work may also address the performance of the movable control surfaces for sway, yaw, roll, pitch, and heave motions. This will in turn permit study of the guidance system to be used on the Towed Body.

APPENDIX MATLAB PROGRAM FILES

A. CALCULATING HYDRODYNAMIC DERIVATIVES

1. Body of Revolution Hydrodynamic Derivatives (bodyspec.m)

```
%LT Scott D. Roberts
%Body Specifications for Towed Body USV retrieval system
%Reference Principles of Naval Architecture Volume III and SLICE Thesis
%20 January 2005

%Body Dimensions
L = 5;                %length in feet
T = 1.111;            %draft in feet (actually diameter of body of
rotation)
xG = 0;               %longitudinal center of gravity

%Hydrodynamic Derivatives for Body -- Nondimensional
%From ... SLICE table 1
Yvh = -0.005948;
Nvh = -0.012795;
Yrh = 0.001811;
Nrh = -0.001597;
Yvdoth = -0.013278;
Nrdoth = -0.000676;
Yrdoth = 0.000060;
Nvdoth = 0.000202;

%data extrapolated from table 3 of stability and control derivatives
for DSRV -- Nondimensional
mfactor = -0.97675;
Izfactor = -0.79532;

m = Yvdoth/mfactor;
Iz = Nrdoth/Izfactor;
```

2. Fin Specifications (rudderspec.m)

```
%LT Scott D. Roberts
%Rudder Specificiations for Towed Body USV retrieval system
%Reference Principles of Naval Architecture Volume III
%20 January 2005

ar = a/2;             %geometric aspect ratio
sweep = 0;            %sweep angle of the quarter-chord line
Cdc = 0.8;            %crossflow drag coefficient dependent on both tip
shape and taper ratio
Cdo = 0.0065;         %for NACA 0015
e = 0.90;             %Oswald efficiency factor
taper_ratio = 0.45;
bbar = croot*ar;      %span width in feet
ctip = croot * taper_ratio; %length in feet
cbar = (croot + ctip)/2;    %mean chord length
Arud = (croot+ctip)*bbar/2; %rudder area
```

3. Total Hydrodynamic Derivatives for Towed Body (hydroderiv.m)

```
%LT Scott D. Roberts
%Total Hydrodynamic Derivatives for Towed Body and Rudder
%Reference Principles of Naval Architecture Volume III, page 242
%20 January 2005

%%%%%%%%%%%% Access data for towed body and rudder
bodyspec
rudderspec
%%%%%%%%%%%%
b = bbar;            %rudder span length in feet
A1f = Arud/(L*T);    %nondimensional Arud
xF1 = xF/L;          %nondimensional xF
b1 = b/L;            %nondimensional b
croot1 = croot/L;    %nondimensional croot

%Hydrodynamic Derivatives for Rudder -- Nondimensional
Yvf = -abs(A1f*pi/2*a);
Nvf = Yvf*xF1;
Yrf = xF1*Yvf;
Nrf = (xF1)^2*Yvf;
Yvdotf = -(4*pi*b1*A1f)/(a^2+1)^(1/2);
Nrdotf = xF1*Yvdotf;
Yrdotf = xF1*Yvdotf;
Nvdotf = (xF1)^2*Yvdotf;

%Total Towed Body Derivates -- Nondimensional
Yv = Yvh + n*Yvf;
Nv = Nvh + n*Nvf;
Yr = Yrh + n*Yrf;
Nr = Nrh + n*Nrf;
Yvdot = Yvdoth + n*Yvdotf;
Nrdot = Nrdoth + n*Nrdotf;
Yrdot = Yrdoth + n*Yrdotf;
Nvdot = Nvdoth + n*Nvdotf;
```

4. Stability Criteria Calculations (stability.m)

```
%LT Scott D. Roberts
%Towing Stability Criteria for Towed Body
%Reference:  Latorre and Bernitsas
%28 January 2005

%Call data from hydrodynamic coefficient m.file
hydroderiv
ro = 64.1;  %standard seawater density in lb/ft^3
u0 = 8.439; %tow vessel speed in ft/sec
U = u0;     %towed body speed
U1 = U/u0;  %nondimensionalized towed body speed
xp = 2.4;   %distance in feet from center of body to tow point at front
of body
xp1 = xp/L; %nondimensionalized
l = 328;    %length in feet of unstrained towline
l1 = l/L;   %nondimensionalized
T = 1000;   %Tension in towline in lbf
```

```
T1 = T/((ro/2)*L^2*u0^2);   %nondimensionalized

%Characteristic equation coefficients
A = (Yvdot - m)*(Nrdot - Iz) - Nvdot*Yrdot;
B = (Yvdot - m)*(Nr - Nvdot*U1) + Yv*(Nrdot - Iz) + (Yvdot*U1-Yr)*Nvdot
- Yrdot*Nv;

A0 = A;
B0 = B;
C0 = Yv*Nr + Nv*(m-Yr);
C1 = (m-Yvdot)*xp1 + Nvdot;
C2 = -(Nrdot - Iz) + (m-Yvdot)*(xp1)^2 + xp1*(Nvdot+Yrdot);
C = C0 + T1*(C1 + C2/l1);
D1 = Nv - Yv*xp1;
D2 = -Yv*(xp1)^2 + Nv*xp1 + (Yr+Yvdot)*xp1 - Nr + Nvdot;
D = T1*(D1+D2/l1);
E2 = D1;
E = (T1/l1)*E2;

alpha1 = (B0*C1*D1 - A0*(D1)^2) + (1/l1)*(B0*C1*D2 + B0*C2*D1 -
2*A0*D1*D2) + (1/(l1)^2)*(B0*C2*D2-A0*(D2)^2);
alpha2 = B0*C0*D1 + (1/l1)*(B0*C0*D2 - (B0)^2*E2);

Gh = 1-((Nv*(Yr-m))/(Yv*(Nr-m*xG)));

%Active Criteria
R1 = [xp1 (Nv/Yv)];
R2 = [T1 (-alpha2/alpha1)];

if R1(1) > R1(2)
    cond1 = 1;
else
    cond1 = 0;
end

if R2(1) > R2(2)
    cond2 = 1;
else
    cond2 = 0;
end
```

5. Variable Range Assignment and Data Collection (variables.m)

```
%LT Scott Roberts
%Program Run sequence for all values of n, a, croot, and xF
%01 February 2005

clc,clear
datav = [];
datanf = [];
for n = 1.0:1:2.0
    for a = 0.5:0.5:6.0
        for xF = -0.2:-0.1:-2.5
            for croot = 0.1:.05:1.5
```

```
                stability;
                datav = [datav; n a xF1 croot1 R1(1) R1(2) R2(2) cond1
Gh];
            end
        end
    end
end
n = 0;
for croot = 0.1:0.05:1.5
    stability;
    datanf = [datanf; n a xF1 croot1 R1(1) R1(2) R2(2) cond1 Gh];
end
```

LIST OF REFERENCES

Bernitsas, M. and Kekridis, N., "Simulation and Stability of Ship Towing", ISP, Volume 32, No. 369, May 1985

Gourley, Scott R., "Revamped Matagorda: A Sign of Things to Come," The United States Coast Guard: The Shield of Freedom – A Government Services Group Publication, A Division of Faircount LLC, June 2004.

Healey, Anthony J., "Dynamics and Control of Mobile Robotic Vehicles", Naval Postgraduate School, Monterey, CA, 2001.

Healey, Anthony J., "Dynamics and Control for UUVs", Naval Postgraduate School Center for AUV Research, Monterey, CA, May 2002.

Latorre, Robert, "Development of Data for Extended Linear Analysis of Towed Vessel Performance", School of Naval Architecture and Marine Engineering, University of New Orleans, LA, July 1984.

Mulhern, F. Mark, Ship Systems Engineering Station Philadelphia (SSES), Phone Call, November 2004.

Naval Surface Warfare Center Carderock Division, "Surface Combatant Optimized for Unmanned Vehicle Operations (SCOUVO)", Innovation Center Technical Report NSWCCD-INCEN-TR-2003/001, West Bethesda, MD, September 2003.

Navy TACMEMO 3-22-5-SW, "Integration of Unmanned Vehicles into Maritime Missions."

Papoulias, F., "TS4001: Maneuvering Notes", Naval Postgraduate School, Monterey, CA, 2004.

Principles of Naval Architecture, Volume III, Edward V. Lewis editor, Society of Naval Architects and Marine Engineers, 1989.

Sarch, M., "Fin Stabilizers as Maneuver Control Devices," Master's Thesis, Naval Postgraduate School, Monterey, CA, December 2003.

Sheinberg, Rubin, Christopher Cleary and Thomas Beukema, "Worldwide Assessment of Stern Launch Capability" 24th United States Japan Cooperative Program in Natural Resources (U.S./UJNR), *Marine Facilities Panel Meeting*, Honolulu, HI, November 2001.

Wolkerstofer, William J., "A Linear Maneuvering Model for Simulation of SLICE Hulls," Master's Thesis, Naval Postgraduate School, Monterey, CA, 1995.

Young, D.B., "Model Investigation of the Stability and Control Characteristics of the Contract Design for the Deep Submergence Rescue Vehicle (DSRV)", Naval Ship Research and Development Center, Washington, D.C., April 1969.

INITIAL DISTRIBUTION LIST

1. Defense Technical Information Center
   Ft. Belvoir, Virginia

2. Dudley Knox Library
   Naval Postgraduate School
   Monterey, California

3. F. Mark Mulhern
   Ship Systems Engineering Station
   Philadelphia, Pennsylvania

4. William Solitario
   Naval Postgraduate School
   Monterey, California